

Validation of Slosh Model Parameters and Anti-Slosh Baffle Designs of Propellant Tanks by Using Lateral Slosh Testing

José G. Pérez

Russel A. Parks

Daniel R. Lazor

NASA Marshall Space Flight Center, Huntsville, AL

ABSTRACT

The slosh dynamics of propellant tanks can be represented by an equivalent mass-pendulum-dashpot mechanical model. The parameters of this equivalent model, identified as slosh mechanical model parameters, are slosh frequency, slosh mass, and pendulum hinge point location. They can be obtained by both analysis and testing for discrete fill levels. Anti-slosh baffles are usually needed in propellant tanks to control the movement of the fluid inside the tank. Lateral slosh testing, involving both random excitation testing and free-decay testing, are performed to validate the slosh mechanical model parameters and the damping added to the fluid by the anti-slosh baffles. Traditional modal analysis procedures were used to extract the parameters from the experimental data. Test setup of sub-scale tanks will be described. A comparison between experimental results and analysis will be presented.

KEY WORDS: baffle, fluid, model, propellant, slosh, sub-scale

INTRODUCTION

The slosh phenomenon may be defined as oscillations of the free surface of a fluid on a partially filled container. These oscillations may be caused by several sorts of perturbations, such as external forces, motions, and displacements. The magnitude of fluid sloshing depends on the container geometry, fluid properties, fluid fill level, perturbing motion of the container, acceleration field and damping capability of the system (NASA SP-8009). If the sloshing of propellants is not properly controlled, it may affect the stability and structural integrity of space vehicles.

The dynamic response of a vehicle to propellant sloshing can be calculated by using an equivalent mechanical model to represent the fluid dynamics (Abramson et al. 1966). Those models may consist either of mass-pendulum-dashpot systems, or mass-spring-dashpot systems, and are designed so that they have the same resultant pressure force, moment, damping, and frequency as the actual systems (NASA SP-8009).

The slosh mechanical model is one of the several inputs incorporated in the stability and structural analyses of space vehicles. Once these analyses are performed, minimum damping requirements for stable flight control are issued.

The damping requirements are often met with the addition of flat rings attached to the inside of the tank walls. The flat rings are called anti-slosh baffles, and serve to control the slosh

oscillations of the propellant. A semi-empirical equation, known as Miles equation (Miles 1958), is used to predict the damping added by these rings to the propellant.

Testing involving different fluids on full scale and sub-scale tanks provided the basis for the development of the analysis tools used in slosh dynamics: the slosh mechanical model and Miles equation. Lateral slosh in cylindrical tanks has been extensively studied and compared to experimental data (Abramson et al. 1966).

Historically, it has been a requirement for NASA programs, such as the Apollo, the Space Shuttle, the Ares, and currently the Space Launch System, to verify the stable flight control damping requirements, which involves validating the slosh mechanical model, and investigating the damping added by different components inside the tank, such as anti-slosh baffles. Validation is needed because analytic uncertainty exists with fluid response in curved surface regions of tanks with domed tops or bottoms versus pure cylinders (Abramson et al. 1966). This validation is accomplished by performing lateral slosh tests in sub-scale models of the prototype tanks using water to simulate the propellant, in 1g conditions.

This paper is based on a preliminary assessment of the lateral slosh tests performed to validate the slosh mechanical model and baffle designs for the Ares I Upper Stage (US) Liquid Oxygen (LOX) and Liquid Hydrogen (LH2) tanks. The tests were performed in 1/5 scale models of the tanks, and were designed to validate the analytical models and to identify possible limitations in the analysis tools (Parks, Lazor and Lacock 2011a).

LINEAR MECHANICAL MODEL OF PROPELLANT SLOSHING

A linear mechanical model of propellant sloshing was used to analyze the slosh dynamics of the Ares I US tank models. The mechanical model consists of a fixed mass, and one or more slosh masses connected to pendulums and dashpots. The number of slosh masses included in the model corresponds to the number of slosh modes considered in the analysis. For axi-symmetric tanks usually only the first mode creates significant slosh loads (Dodge and Abramson 2000), the influence of the higher modes being often negligible in comparison with the first mode. Only first mode parameters are going to be reported in this document. A schematic of the model is shown in Figure 1.

The slosh mass, as the name implies, is the mass involved in the sloshing. The fixed mass is the mass that does not take part in the sloshing. For a given fill level, the total fluid mass (m) is the addition of the fixed mass (m_F) and the slosh mass (m_S). The parameters of interest from the slosh linear mechanical model are the slosh frequency (f_S), the slosh mass (m_S), and the pendulum hinge point location (H_S). These parameters are determined for different fill levels, and are needed to perform stability analyses. The rest of the parameters can be derived from these. Equations 1 through 4 are used to determine the slosh model parameters for the first slosh mode in cylindrical tanks (Abramson et al. 1966).

In the equation, the damping factor δ is defined as:

$$\delta = \frac{1}{n} \ln \left(\frac{x_0}{x_n} \right) \quad (6)$$

As shown in Equation (6), a logarithmic decrement may be used to obtain the damping factor either from a slosh force decay curve, or from a slosh wave decay curve. The amplitude of the slosh force or the slosh wave at a given cycle is represented by the letter x . The number of cycles over which the decay is measured is represented by the letter n . The amplitude of a selected initial moment is x_0 , and the amplitude of a selected terminal moment after n cycles is x_n (Stephens, Leonard, and Silveira 1961). The % critical damping is obtained by multiplying the damping ratio ζ by 100.

Dashpots are commonly introduced in the model to represent the viscous damping of the propellant, or damping elements such as baffles (Mason and Starin 2005). The dashpot damping in a tank without baffles may be obtained in several ways. One way is by testing the prototype tank. By using this approach both, the damping provided by the interaction between the fluid and the tank wall, and the damping provided by small structures inside the tank (such as stringers, ortho-grid, iso-grid, etc.) can be obtained (Bugg 1973). This method usually yields damping values of the order of tenths of a percent (e.g., 0.2% in Bugg 1973). Another option is to use a general equation of smooth-wall damping, which only considers the effect of the interaction between the fluid and the tank wall.

SMOOTH-WALL (“VISCOUS”) DAMPING

The smooth-wall damping is the damping produced by the interaction between the fluid and the tank wall. The magnitude of the smooth-wall damping has been determined for several configurations. In tanks of various geometries without baffles, it may be described by a semi-empirical equation of the form (Abramson et al. 1966):

$$\zeta_{SW} = \frac{4.98}{2\pi} \sqrt{\frac{\nu}{R^{1.5} g^{0.5}}} \left[1 + \frac{0.318}{\sinh(1.84h/R)} \left(1 + \frac{1 - (h/R)}{\cosh(1.84h/R)} \right) \right] K \quad (7)$$

In the equation, ζ_{SW} is the smooth-wall damping (also known as “viscous damping coefficient”), ν is the kinematic viscosity of the liquid, and K is a numerical coefficient that takes on different values depending upon tank geometry and fill level. For a cylindrical tank, $K = 1$.

For a spherical tank:

$$K = (R/h) \text{ for } 0 \leq h \leq R \quad (8)$$

and:

$$K = \frac{[1 + 0.46(2 - h/R)]}{[1.46(2 - h/R)]} \text{ for } h \geq R \quad (9)$$

For a cylindrical tank with a spherical bottom (center of sphere inside the tank), Equation (8) can be used for $0 < h \leq R$, and $K = 1$ for $h \geq R$. More information about the values of coefficient K for other tank geometries can be obtained from references (Abramson 1969, Ibrahim 2005).

BAFFLE (“DRAG”) DAMPING AND MILES EQUATION

Baffles usually need to be placed at the tank walls to provide the damping required to meet stability requirements and prevent instabilities in the control system (Figure 2). Baffles are more effective if they are positioned perpendicular to the flow streamlines in the tank. Flat ring baffles is the most efficient (Silveira, Stephens and Leonard 1961) and most frequently used (Abramson 1969) slosh-suppression system in cylindrical tanks, although there are other types of baffles, such as conical baffles, cruciform baffles, and radial baffles, that may be more appropriate for certain applications.

The baffle damping is determined by using Miles equation (Miles 1958, Roberts, Basurto and Chen 1964, Dodge 2000). This semi-empirical equation is based on research on fluid drag in flat plates (Keulegan and Carpenter 1956). Test data show that the damping reaches a peak value when the baffle is located just slightly below the undisturbed fluid free surface, decreasing sharply for other baffle depths. For flat ring baffles in a tank, the damping estimated from Miles equation (Dodge 2000) is:

$$\zeta_{Miles} = \frac{15 (4/3\pi)^2 \alpha A e^{-4.601d/R} \sqrt{\eta w}}{2 \sqrt{\pi} (m_s/\rho) \Gamma^2} \quad (10)$$

where ζ_{Miles} is Miles equation baffle damping, d is the depth of the baffle below the undisturbed fluid free surface, A is the tank cross-sectional area, η is the slosh wave amplitude at the tank wall (the amplitude of the liquid oscillations measured at the tank wall from the undisturbed fluid free surface, as shown in Figure 1), w is the baffle width, ρ is the propellant density, Γ is the ratio of the lateral displacement of the slosh mass to the slosh wave amplitude (depends on the tank shape), and α is the fraction of the tank cross-sectional area covered by the baffle (ratio of the baffle area to the tank cross-sectional area), defined in a tank of a circular cross-section as:

$$\alpha = \frac{2w}{R} - \frac{w^2}{R^2} \quad (11)$$

For cylindrical tanks, the damping of a series of ring baffles is calculated on the basis of linear superposition. As spacing between the baffles become less than one baffle width, the superposition does not accurately predict damping (Abramson 1969). For the commonly used cylindrical tank, a good design principle is spacing the ring baffles at a distance $s \leq 0.2R$. The design of anti-slosh flat ring baffles is based on selecting baffle width, spacing, and depth to produce the required minimum damping (Abramson 1969).



Figure 2: Anti-Slosh Flat Ring Baffles in the Ares I US LH2 Tank Model.

MODEL TO PROTOTYPE SCALING

When the slosh mechanical model parameters are determined empirically by sub-scale model testing only, similitude analysis should be performed to obtain the parameters for full-scale prototype dimensions and properties (Abramson and Ransleben 1960). Complete dimensional analysis shows that the model masses are scaled in proportion to the total liquid mass, and all length dimensions are scaled geometrically (Dodge and Garza 1969). For a geometrically scaled tank, one of the most important scaling parameters is the Froude number (Abramson et al. 1966) which states that all frequencies are scaled in proportion to $g^{0.5}/R^{0.5}$ (Unruh et al. 1986). The smooth-wall damping is roughly proportional to $v^{0.5}/R^{0.75}g^{0.25}$, a factor analogous to Galilei number and Reynolds number. Drag damping due to baffles, for geometrically scaled baffles and slosh wave amplitudes, generally scales one-to-one in terms of log decrements between sub-scale model and full-scale prototype (Abramson et al. 1966, Dodge and Garza 1969, Unruh et al. 1986).

The primary advantage of experimentally determining the parameters of the slosh mechanical model is that the force and moment response of the sub-scale model tests can be used to determine mechanical model parameters which, when suitably non-dimensionalized, are valid for both model and prototype (Dodge and Garza 1969). Test results and analyses in this document are presented in non-dimensionalized form parameters when possible, as listed in Table 1, where ω_S is the circular frequency ($\omega_S = 2\pi f_S$, in radians/s). The only exception will be the smooth-wall damping, which will be shown as is obtained from the model tests, so it can be directly compared with the baffle damping data obtained from the model tests. Although baffle damping scales one-to-one for geometrically similar baffles and slosh wave amplitudes, the magnitude of smooth-wall damping will be smaller for the prototype tanks due to the size of the full-scale tanks and the propellant properties.

Table 1: Parameters in Non-Dimensionalized Form.

| Parameter | Original | Non-Dimensionalized |
|----------------------|-----------------|--|
| Fill Level | h | h/R |
| Slosh Frequency | f_S | $\omega_S R^{0.5}/g^{0.5}$ |
| Slosh Mass | m_S | m_S/m |
| Pendulum Hinge Point | H_S | H_S/R |
| Viscous Damping | ζ_{SW} | $\zeta_{SW} R^{0.75} g^{0.25} / \nu^{0.5}$ |
| Drag Damping | ζ_{Miles} | ζ_{Miles} |

TEST METHODS

Lateral slosh testing of 1/5 scale Ares I US LOX and LH2 tank models was conducted at NASA Marshall Space Flight Center. As stated before, the purpose of these tests was to acquire test data for the validation of the analysis tools used to obtain the parameters of the slosh mechanical model, and to estimate baffle damping. To validate Miles equation for baffle damping, testing was conducted with baffles installed in a variety of configurations in the tank models, with varying water levels, to determine their damping effect on the fluid. Series tested on the tank models included configurations involving the empty tank, single baffles and multiple baffles. De-ionized water was used in all tests.

Historical research of slosh test programs shows that the most straight forward and effective way to measure the slosh mechanical model parameters is to configure the tank in a fixture that is rigid in the bandwidth of interest (Green, Walter and Burkey 2005). The fixture can then be driven in different ways to excite the fluid slosh modes. Force sensors can be embedded in that fixture to measure forces caused by the sloshing of the test fluid. These forces can be post-processed and translated to a six degree-of-freedom (6 DOF) force measurement and used in conjunction with fixture accelerations to calculate apparent mass and effective mass-moment functions. The values and properties of these functions can then be used to calculate the required slosh mechanical model parameters (Unruh et al. 1986). This test method is called random excitation (RE) testing.

Another method is to excite the same fixture with a sinusoid input at the slosh fundamental frequency. When the slosh waveform is built up to a desired slosh wave amplitude on the tank wall, the oscillatory motion of the tank is quick-stopped at a point as close to zero velocity as possible to minimize transient inputs. The residual horizontal slosh force decays are recorded (Sumner, Shramo and Stofan 1964). This time data is then post processed to determine the parameters of interest. This test method is called free decay (FD) testing. A limitation of this method is the inability to directly calculate the slosh mass from the acquired data.

Random excitation testing was used in cases in which slosh mass was of interest. A continuous random input of 0.1-3.2 Hz was used. Data from these tests were used to determine slosh frequency, slosh mass, pendulum hinge point location, and smooth-wall damping. These parameters were estimated for first slosh modes and most of the second slosh modes.

Free decay testing was used to evaluate nonlinear behavior and damping dependency on slosh wave amplitude. In general, excitation was applied as close as possible to the frequency of the first slosh mode. Any significant divergence from the natural frequency caused a “beating” effect on the slosh wave and made it difficult to achieve a steady-state slosh wave. Excitation was increased slowly until a steady state slosh wave amplitude was achieved (typically ½, 1, or 2 inches). The table was then hard-stopped at a point as close to zero velocity as possible to minimize transient inputs. The hydraulic shaker used to apply the excitation was then used to hold the fixture rigid. A mechanical stop was also implemented to assure that the fixture was held as rigid as possible. Throughput data was acquired at a 100 Hz sample rate during excitation and free decay. This data was post-processed to determine slosh frequency, pendulum hinge point location, and slosh wave amplitude damping.

It is important to mention that when these series of lateral slosh tests started, in some tests there was an observed slow change in slosh direction during the free decay of the slosh wave, particularly in the no baffle configurations. This change in slosh direction is referred to as “swirl”. There are many hypotheses on the cause of swirl, but it is believed that the major contributor in the case of these tests is a preferred orientation of the slosh. The preferred slosh direction could be caused by a slight out-of-roundness of the tank. Care was taken to orient the tanks to minimize swirling. Another potential cause of swirling was the tank filling process. Due to the tank filling process, a circular flow was developed in the tank. If this flow was not allowed to die out before a test, swirling was observed. The major concern for swirl was its effects on damping measurements since damping was calculated in the axis of excitation. When the fluid is swirling, the kinetic energy effectively decreases from the excitation axis and the slosh wave rotates off of this axis. For this reason, the damping values estimated with swirl will appear higher than if damping values were estimated in the same configuration without swirl. Swirling could be characterized by viewing the free decay data in both lateral directions.

TEST BED, FIXTURE, AND INSTRUMENTATION

Testing was conducted at MSFC in a test bed specifically developed for these tests. The main elements of the test fixture are shown in Figure 3. A rigid aluminum plate was grouted to the concrete floor. Linear rails were bolted to this rigid aluminum plate. A mounting slip plate was attached to these rails with linear bearings. This mounting slip plate provided a “free-sliding” slip table. A fixture consisting of a base plate, support legs, and a tank support ring was bolted to this slip table. The tank support ring was attached to the support legs through three tri-axial ring type force sensors to measure forces due to fluid sloshing and fixture mass. DC capacitive accelerometers in a tri-axial configuration were placed on each support leg to measure the inputs to the tank. An LVDT was attached to the slip table to measure table displacements. Excitation was applied to the slip table by a hydraulic shaker. A dynamic load cell was used to measure the force inputs to the slip table. The test bed and fixture installed, and the test coordinate system are shown in Figure 4.

Water fill levels in the tank were measured using two methods. The first method was a real-time measurement using an ultrasonic distance sensor. This sensor was screwed into a hole manufactured in the top of the tank lid. The second method to measure the water fill levels was by using a rod. For this method, an initial measurement was made from the very top of the tank

to the bottom of the tank. This measurement was made through the same hole that the ultrasonic sensor was mounted. A rod was then used to measure the distance from the top of the tank to the water level. Marks were placed on the rod using a caliper to locate distances needed for the specified water heights. The rod was supported on the top of the tank using a clamp placed at the marks.

Video data was acquired to determine slosh wave amplitudes and capture overall characteristics of the slosh waves during test. A camera was used to capture the slosh free decay. These videos were post-processed to determine slosh wave amplitudes. Due to the optical distortions of the thick walled tank the video needed to be calibrated for the true water level in the tank. To do this, a calibration video was acquired while draining the tank and taking a water level measurement with the ultrasonic sensor. A monitor displaying the ultrasonic sensor measurement was placed in the video as shown in Figure 5. A video calibration could then be calculated by determining water level pixel locations and coinciding ultrasonic sensor measurements. Standard video was acquired from two orthogonal surveillance cameras capturing the overall slosh wave characteristics.

The data acquisition system (DAS) was controlled by a Windows laptop workstation.

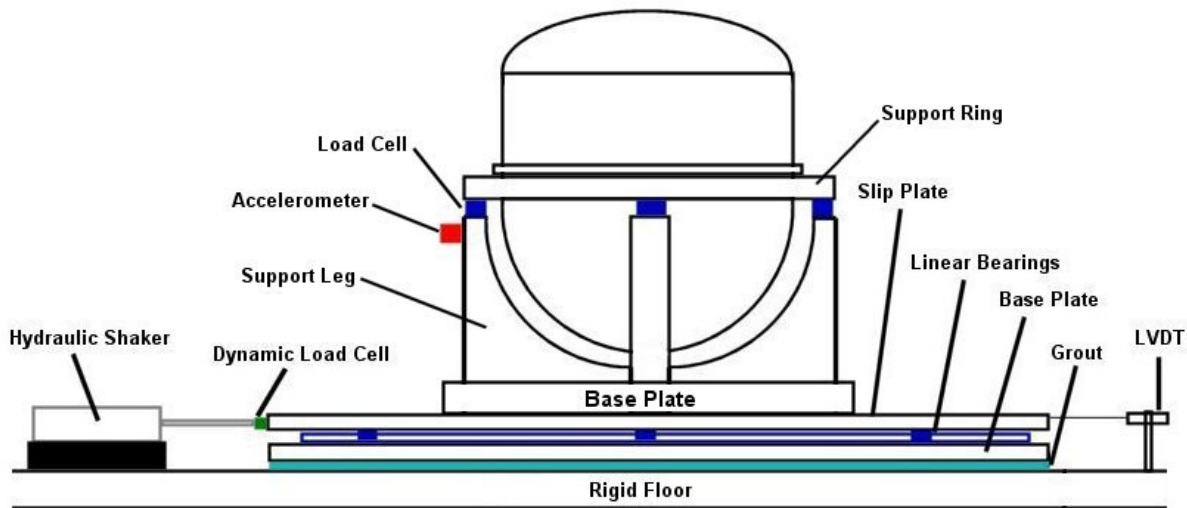


Figure 3: Test Bed Layout.

TEST FIXTURE 6-DOF FORCE TRANSFORMATION

As previously mentioned, it is desirable to have a single point 6 DOF load measurement in the center of the fixture at some height that can be calculated from the nine force outputs from the three tri-axial load cells in the fixture. This calculation is facilitated by developing a force transformation matrix. To do this, a structure with known mass, center of gravity and moment of inertia properties was configured in the fixture as shown in Figure 6. The fixture was then supported in a free-free condition as shown in Figure 7. In this application the fixture was supported by bungee cords by an overhead crane. The calibration mass was then instrumented

with accelerometers. The fixture was impacted on the fixture side of the load cells and data was acquired from the accelerometers and load cells. A single point inside the fixture was chosen as a reference, and using rigid body dynamics the accelerations are transformed to an equivalent 6 DOF acceleration at that point. The mass properties of the calibration mass at that point are known. These two quantities give an expected 6 DOF force measurement at the chosen reference point due to the impacts. A force transformation matrix was then calculated between the nine measured forces and the expected 6 DOF forces at the chosen reference point in the fixture. A more in depth description of the theory and the process is located in the references (Parks, Lazor and Lacock 2011a, 2011b and 2011c).

The force transformation matrix developed for this test proved to be crucial in measuring and calculating the slosh parameters of interests. One of the reasons for this was the inherent flexibilities of the fixture and the effect it had on the nine fluid slosh force measurements. Since the Ares I US LOX tank model had a curved bottom it was necessary to design support legs that allowed for that geometry. For that reason two of the legs, in particular the two farthest from the shaker (Figure 8), had a structural flexibility in the axis of excitation and in the orthogonal direction. This caused cross-coupling forces in the X and Y directions. As a result, reaction forces were measured in both the X and Y directions on those two load cells due to the sloshing fluid. Since the force transformation matrix was developed by testing the fixture in this configuration, this cross-coupling was accounted for in the transformation matrix.

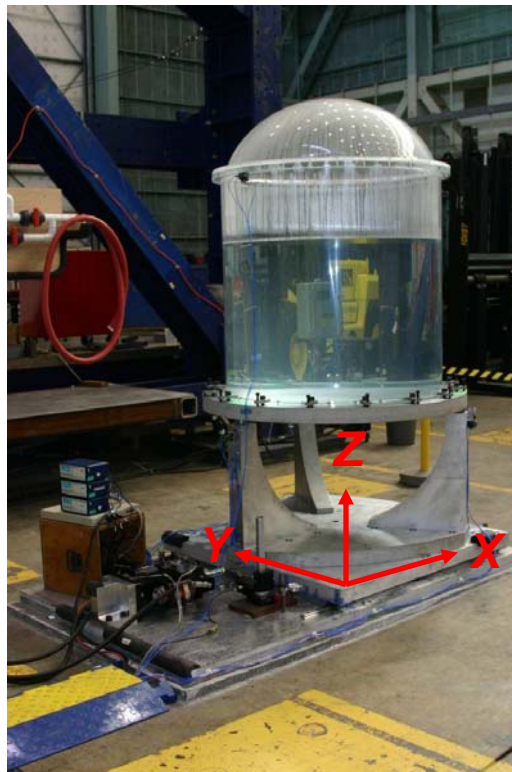


Figure 4: Ares I US LH2 Tank Model Test Setup and Coordinate System.



Figure 5: Video Calibration Image. The dark strip in the center of the picture is the water line, just above the upper flange of the Ares I US LOX tank model.

TEST ARTICLES AND BAFFLES

To enable visualization of the fluid slosh the tanks were made from transparent acrylic (Figures 4 and 8). In the Ares I US LOX tank model, the mounting flange that is used to support the tank in the fixture was designed to hold the tank while filled with water. The tank can not be separated at this location. The upper flanges of both tanks enable the top to be removed. A $\frac{1}{2}$ inch thick aluminum ring (Figure 5) with O-ring groove was placed between the upper flanges of both tanks to prevent water leaks.

Four $\frac{1}{4}$ inch square stainless steel ribs were constructed that matched the curvature of the tanks as close as possible. These ribs were then bolted to the $\frac{1}{2}$ inch aluminum ring in the upper flange and to a 3.59 inch radius, $\frac{1}{4}$ inch thick stainless steel plate at the bottom of the tank. Thin $\frac{1}{4}$ inch thick stainless steel shelves were bolted to these ribs to support the baffles. The baffles were bolted to these shelves. Baffles were made of 0.12 inch thick stainless steel sheets. A configuration of seven baffles is shown in Figure 9.

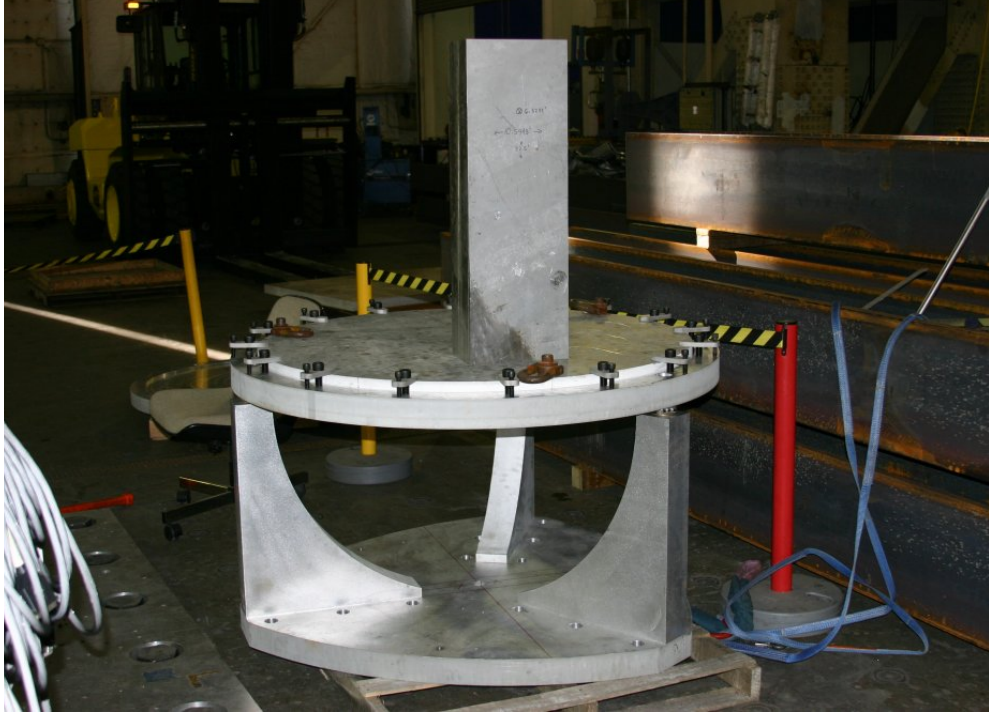


Figure 6: Fixture with Calibration Mass.

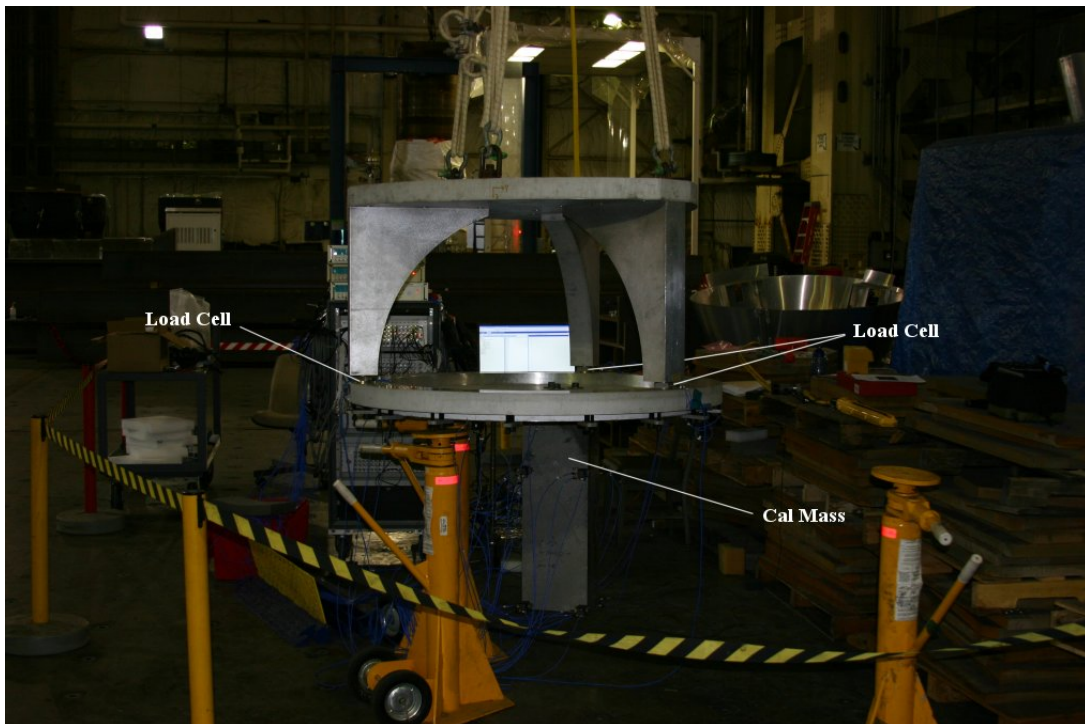


Figure 7: Fixture in Free-Free Condition and Calibration Mass.



Figure 8: Ares I US LOX Tank Model in Test Bed.

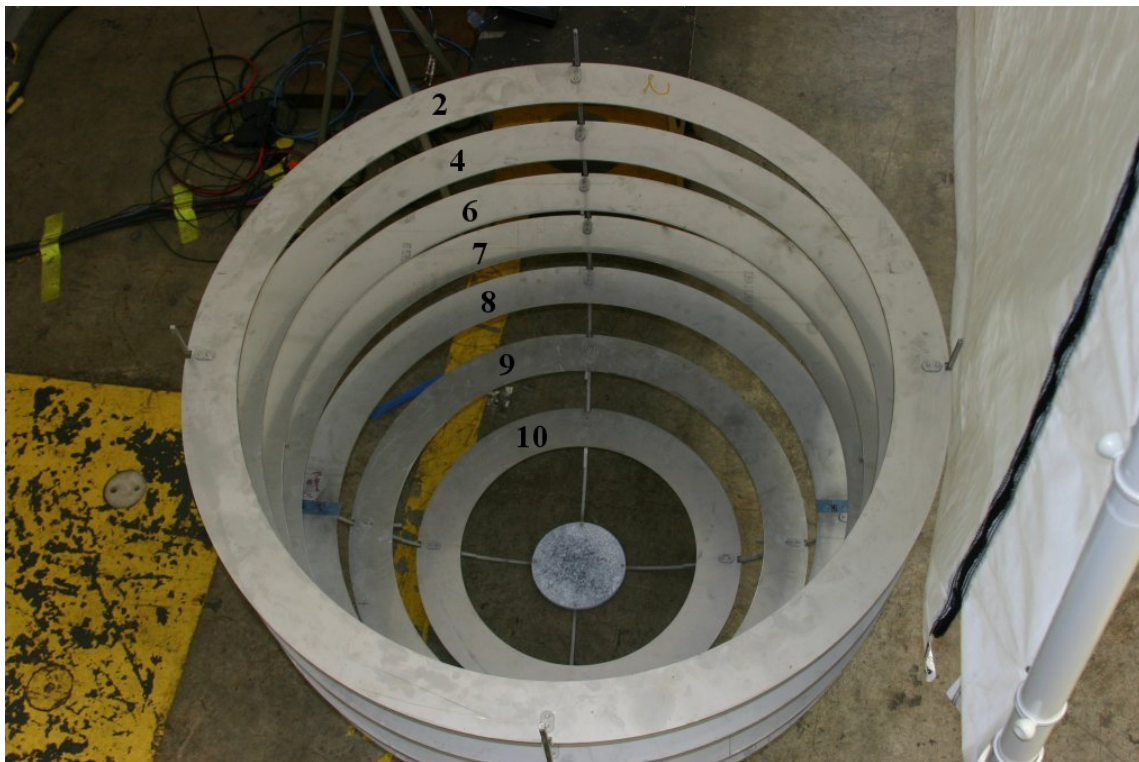


Figure 9: Ares I US LOX Tank Model Baffle Cage.

ARES I US LH2 TANK MODEL DIMENSIONS

The geometrical dimensions of the Ares I US LH2 tank model used for the slosh dynamics analyses were measured directly from the tank and are shown in Figure 10. The tank model consists of a cylindrical barrel section and a spheroidal upper dome. The tank model diameter and upper dome height were scaled approximately 1/5 of the prototype dimensions, but the barrel section height was scaled a lot shorter than the prototype. The tank model was about 43 inches in diameter.

The analyses to obtain the parameters of the slosh mechanical models reported in the current document were performed using a computer code (Dodge 2000), and compared with hand calculations using equations (Abramson et al. 1966). A 750 mL sample of the de-ionized water was weighed at 740 g, resulting in a density of 0.987 g/mL (61.6 lbm/ft³). The kinematic viscosity of water $\nu = 0.001566 \text{ in.}^2/\text{s}$ was obtained from the references (Abramson et al. 1966). These values were used in all the analyses presented in the current document.

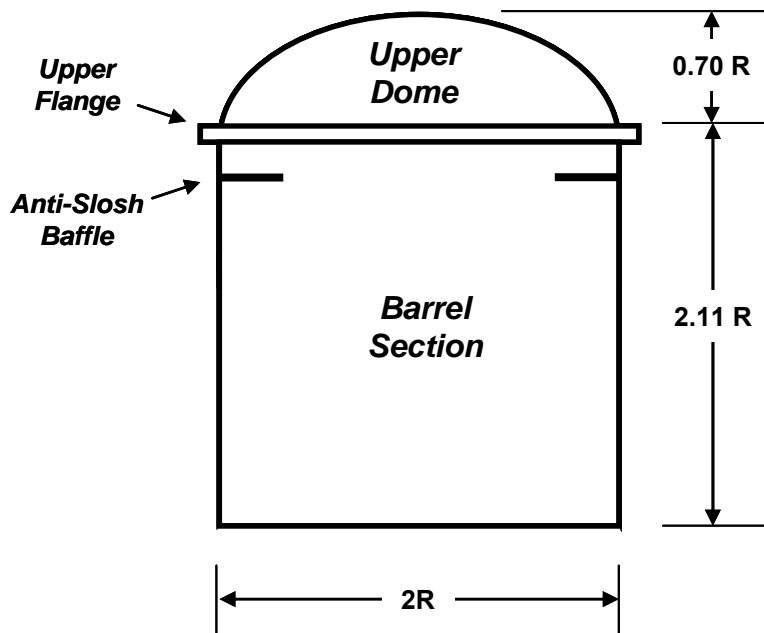


Figure 10: Ares I US LH2 Tank Model Geometry.

ARES I US LH2 TANK MODEL TESTING FOR SLOSH MODEL PARAMETERS

The slosh mechanical model parameters of slosh frequency, slosh mass, and pendulum hinge point location were obtained from random excitation (RE) tests performed on the bare tank (no baffles) (Parks, Lazor and Lacock 2011b).

The analysis and test results of the slosh mechanical model parameters of the Ares I US LH2 tank model are summarized in Tables 2 through 7. The tables correspond to the non-

dimensionalized first mode slosh frequency, first mode slosh mass, and first mode pendulum hinge point location, respectively. To compare analysis and test results, a percent difference with respect to analysis for each fill level tested is also included in all tables. The test results are shown in Figures 11 through 13.

The comparison shows that all the parameters are within the margins used for stability analyses: within 5% for the slosh frequency, and within 15 % for the slosh mass and pendulum hinge point location (Bugg 1997).

Table 2: Ares I US LH2 Tank Model Slosh Frequency RE Test 1.

| fill level h/R | ANALYSIS slosh frequency $\omega_S (R/g)^{0.5}$ | RE TEST 1 slosh frequency $\omega_S (R/g)^{0.5}$ | difference (%) |
|---------------------|--|---|-------------------|
| 0.192 | 0.794 | 0.782 | 1.49 |
| 0.321 | 1.00 | 0.986 | 0.91 |
| 0.385 | 1.07 | 1.06 | 0.99 |
| 0.577 | 1.21 | 1.20 | 0.97 |
| 0.661 | 1.25 | 1.24 | 0.78 |
| 0.745 | 1.28 | 1.27 | 0.82 |
| 0.977 | 1.33 | 1.32 | 0.63 |
| 1.21 | 1.34 | 1.34 | 0.44 |
| 1.39 | 1.35 | 1.35 | 0.37 |
| 1.60 | 1.35 | 1.35 | 0.34 |
| 1.82 | 1.36 | 1.35 | 0.34 |
| 2.08 | 1.36 | 1.35 | 0.79 |
| 2.17 | 1.36 | 1.35 | 0.65 |
| 2.28 | 1.40 | 1.40 | 0.48 |
| 2.44 | 1.55 | 1.54 | 0.75 |

Table 3: Ares I US LH2 Tank Model Slosh Frequency RE Test 2.

| fill level h/R | ANALYSIS slosh frequency $\omega_S (R/g)^{0.5}$ | RE TEST 2 slosh frequency $\omega_S (R/g)^{0.5}$ | difference (%) |
|---------------------|--|---|-------------------|
| 1.30 | 1.35 | 1.33 | 1.64 |
| 1.90 | 1.36 | 1.34 | 1.40 |
| 2.30 | 1.42 | 1.41 | 1.23 |

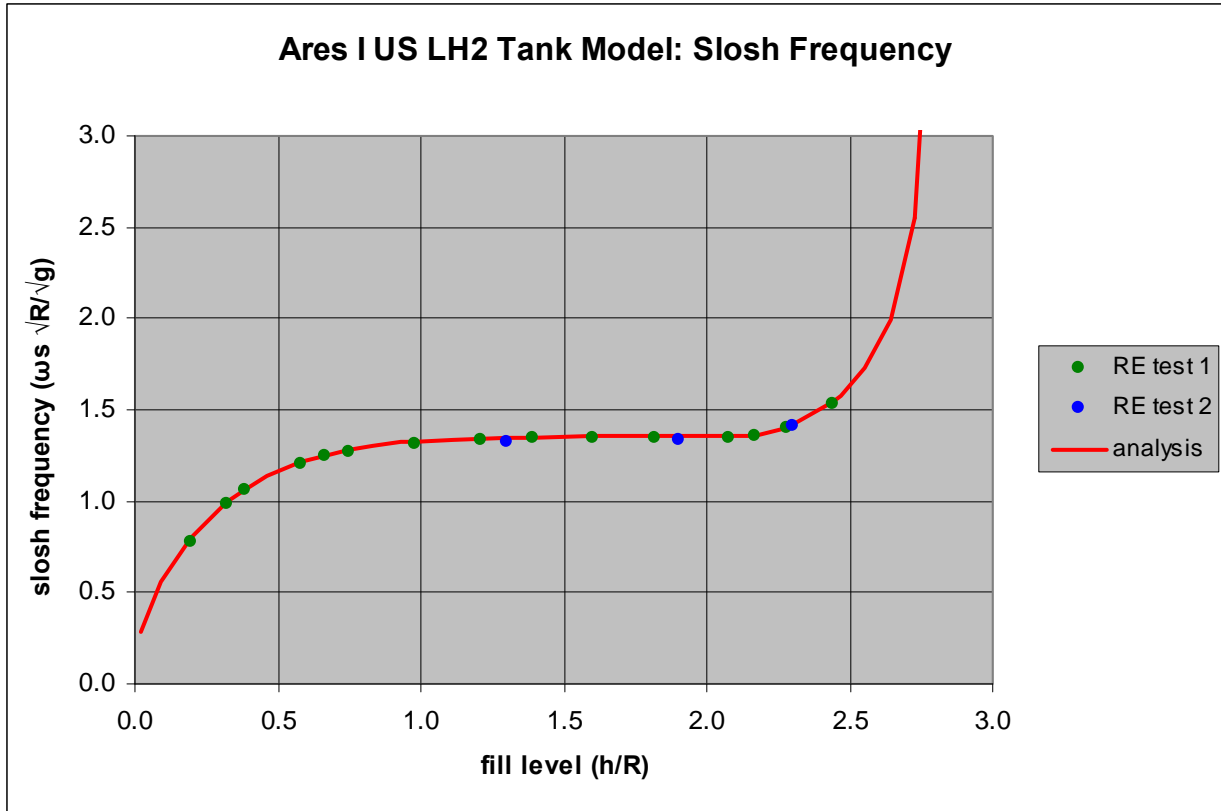


Figure 11: Ares I US LH2 Tank Model Slosh Frequency.

Table 4: Ares I US LH2 Tank Model Slosh Mass RE Test 1.

| fill level <i>h/R</i> | ANALYSIS slosh mass <i>m_s/m</i> | RE TEST 1 slosh mass <i>m_s/m</i> | difference (%) |
|--------------------------|--|---|-------------------|
| 0.192 | 0.809 | 0.801 | 1.00 |
| 0.321 | 0.761 | 0.764 | 0.36 |
| 0.385 | 0.731 | 0.750 | 2.61 |
| 0.577 | 0.630 | 0.599 | 4.98 |
| 0.661 | 0.586 | 0.558 | 4.72 |
| 0.745 | 0.544 | 0.556 | 2.18 |
| 0.977 | 0.445 | 0.448 | 0.68 |
| 1.21 | 0.371 | 0.370 | 0.06 |
| 1.39 | 0.323 | 0.338 | 4.52 |
| 1.60 | 0.282 | 0.290 | 2.87 |
| 1.82 | 0.250 | 0.245 | 1.84 |
| 2.08 | 0.218 | 0.230 | 5.21 |
| 2.17 | 0.208 | 0.212 | 1.50 |
| 2.28 | 0.190 | 0.190 | 0.22 |
| 2.44 | 0.147 | 0.149 | 1.52 |

Table 5: Ares I US LH2 Tank Model Slosh Mass RE Test 2.

| fill level h/R | ANALYSIS slosh mass m_s/m | RE TEST 2 slosh mass m_s/m | difference (%) |
|---------------------|-----------------------------------|------------------------------------|-------------------|
| 1.30 | 0.345 | 0.317 | 8.73 |
| 1.90 | 0.239 | 0.231 | 3.12 |
| 2.30 | 0.184 | 0.190 | 3.33 |

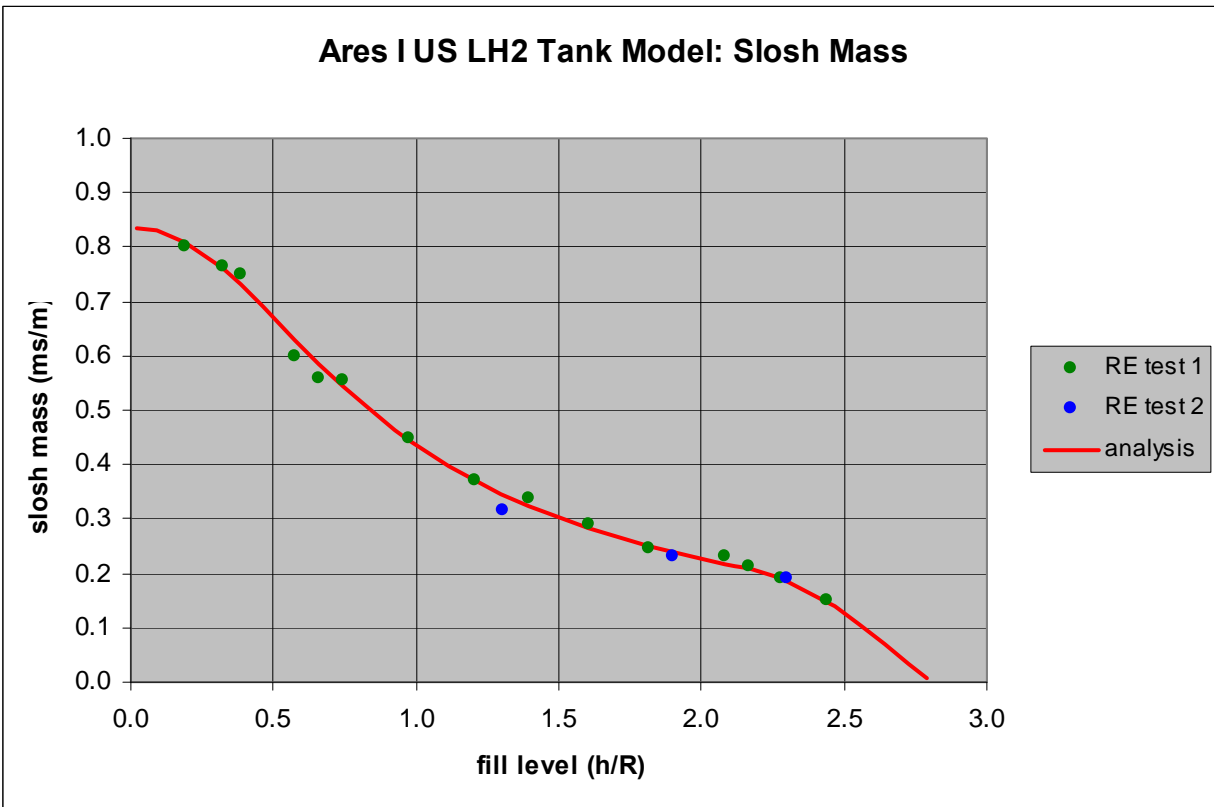


Figure 12: Ares I US LH2 Tank Model Slosh Mass.

Table 6: Ares I US LH2 Tank Model Pendulum Hinge Location RE Test 1.

| fill level h/R | ANALYSIS pendulum hinge point H_S/R | RE TEST 1 pendulum hinge point H_S/R | difference (%) |
|--|---|--|---------------------------|
| 0.192 | 1.59 | 1.52 | 4.31 |
| 0.321 | 1.02 | 1.02 | 0.27 |
| 0.385 | 0.894 | 0.931 | 4.13 |
| 0.577 | 0.732 | 0.744 | 1.64 |
| 0.661 | 0.714 | 0.740 | 3.55 |
| 0.745 | 0.715 | 0.789 | 10.36 |
| 0.977 | 0.781 | 0.847 | 8.44 |
| 1.21 | 0.908 | 0.960 | 6.09 |
| 1.39 | 1.03 | 1.09 | 6.01 |
| 1.60 | 1.19 | 1.28 | 7.34 |
| 1.82 | 1.37 | 1.43 | 4.89 |
| 2.08 | 1.60 | 1.68 | 5.09 |
| 2.17 | 1.67 | 1.78 | 6.59 |
| 2.28 | 1.73 | 1.76 | 2.09 |
| 2.44 | 1.76 | 1.80 | 2.07 |

Table 7: Ares I US LH2 Tank Model Pendulum Hinge Location RE Test 2.

| fill level h/R | ANALYSIS pendulum hinge point H_S/R | RE TEST 2 pendulum hinge point H_S/R | difference (%) |
|--|---|--|---------------------------|
| 1.30 | 0.966 | 1.03 | 5.93 |
| 1.90 | 1.44 | 1.55 | 6.82 |
| 2.30 | 1.73 | 1.87 | 7.58 |

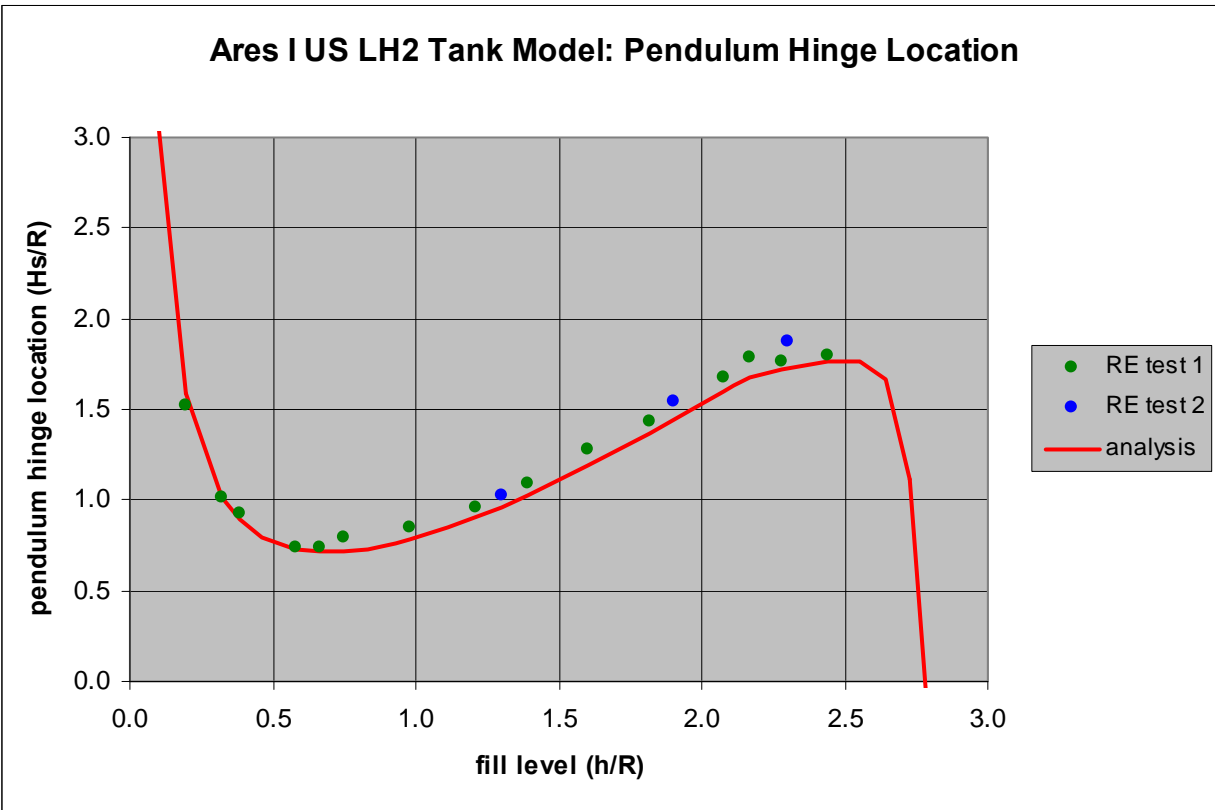


Figure 13: Ares I US LH2 Tank Model Pendulum Hinge Location.

ARES I US LH2 TANK MODEL TESTING FOR SMOOTH-WALL DAMPING

Free decay (FD) tests on the bare tank (no baffles) were performed to estimate smooth-wall damping. Test results and analysis are shown in Table 8 and Figure 14. The first test was performed for a nominal slosh wave amplitude of 1 inch ($\eta/R = 0.0458$), and the second for a nominal slosh wave amplitude of 2 inches ($\eta/R = 0.0916$). No significant difference in the measured smooth-wall damping was observed for the two slosh wave amplitudes tested. As expected, smooth-wall damping is independent of slosh wave amplitude for $\eta/R \leq 0.1$ (Dodge 2000).

Analytical values were obtained from the smooth-wall damping equation for cylindrical tanks (Equation 7). Test results show good agreement with analytical values, although they are consistently higher in the upper dome region. During testing, it was noticed that the ½ inch thick aluminum ring placed between the upper flanges of the tank to prevent water leak was not even with the inside of the tank all the way around. This caused a slight discontinuity at that flange that had some effect on the damping at water fill levels at or just above this area ($h/R = 2.11$).

Table 8: Ares I US LH2 Tank Model Smooth-Wall Damping.

| fill level h/R | ANALYSIS % critical damping ζ_{sw} | FD TEST 1 % critical damping ζ | FD TEST 2 % critical damping ζ |
|---------------------|---|---|---|
| 0.192 | 0.180 | 0.248 | 0.260 |
| 0.321 | 0.127 | 0.170 | 0.154 |
| 0.385 | 0.114 | 0.141 | 0.133 |
| 0.577 | 0.0926 | 0.106 | 0.102 |
| 0.661 | 0.0877 | 0.107 | 0.0950 |
| 0.745 | 0.0841 | 0.0807 | 0.0975 |
| 0.977 | 0.0781 | 0.0690 | 0.107 |
| 1.21 | 0.0751 | 0.0723 | 0.0761 |
| 1.39 | 0.0737 | 0.0714 | 0.0745 |
| 1.60 | 0.0726 | 0.0757 | 0.0767 |
| 1.82 | 0.0719 | 0.0819 | 0.0790 |
| 2.08 | 0.0714 | 0.100 | 0.0947 |
| 2.17 | 0.0713 | 0.114 | 0.0947 |
| 2.23 | 0.0719 | 0.143 | 0.0938 |
| 2.28 | 0.0723 | 0.115 | 0.0814 |
| 2.44 | 0.0778 | 0.136 | 0.108 |

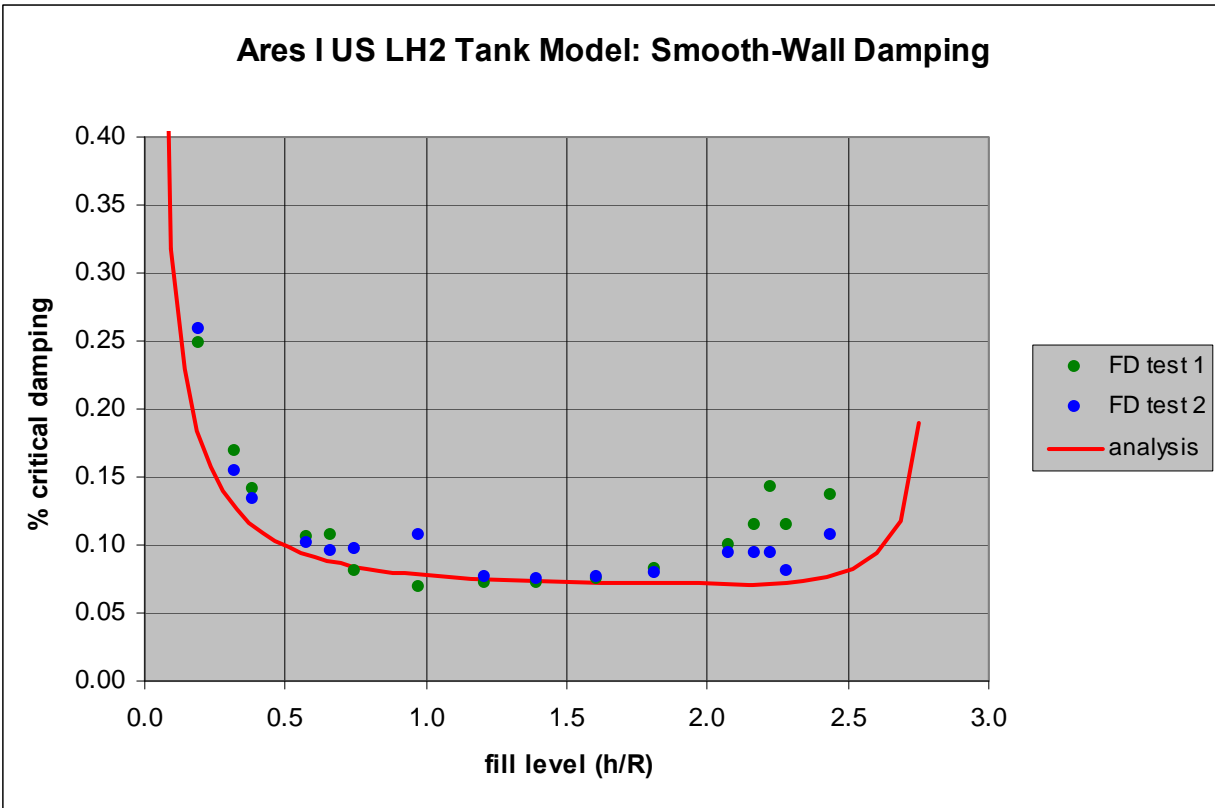


Figure 14: Ares I US LH2 Tank Model Smooth-Wall Damping.

ARES I US LH2 TANK MODEL TESTING FOR BAFFLE DAMPING

Free decay (FD) test results for a single baffle damping are shown in Table 9 and Figure 15. The baffle tested was 4.4 inches wide ($w/R = 0.204$), and was located at a height of 43.91 inches ($h/R = 2.04$). Due to the dependency of the baffle damping on the slosh wave amplitude, only the first two peaks of the force decrement data were considered to obtain the baffle damping values measured from testing.

The analysis curve on Figure 15 was created using Miles equation, in the form shown on Equation 10. For simplicity, the average value of all the slosh wave amplitudes measured during testing of this series ($\eta/R = 0.0585$) was used in the equation to create the analysis curve shown in Figure 15. The agreement between test and analysis is very good.

Table 9: Ares I US LH2 Tank Model Single Baffle Damping.

| fill level h/R | FD TEST % critical damping ζ | FD TEST slosh wave amplitude η/R |
|---------------------|---|--|
| 1.93 | 0.110 | 0.0623 |
| 2.08 | 19.2 | - |
| 2.09 | 20.8 | - |
| 2.11 | 11.0 | - |
| 2.16 | 7.95 | 0.0669 |
| 2.21 | 5.62 | 0.0575 |
| 2.23 | 5.23 | 0.0766 |
| 2.26 | 3.74 | 0.0478 |
| 2.28 | 3.68 | 0.0525 |
| 2.36 | 2.00 | 0.0456 |
| 2.47 | 1.04 | - |

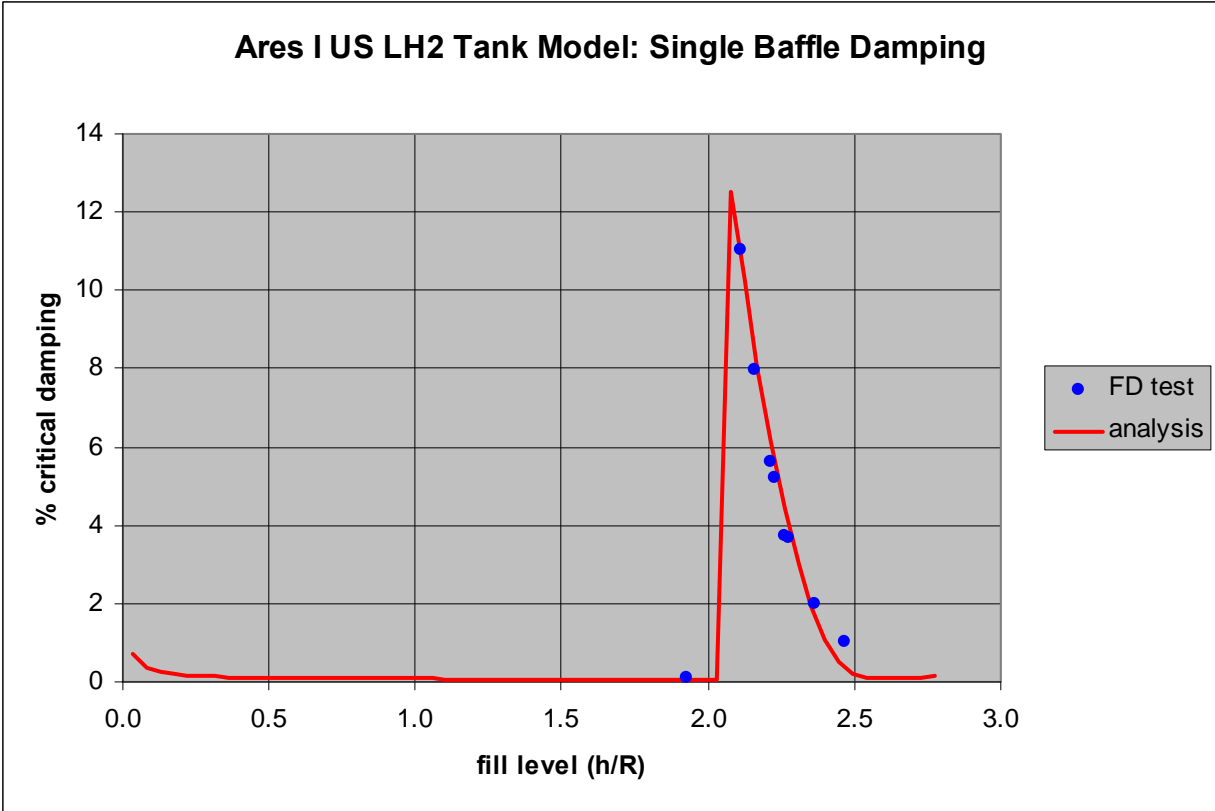


Figure 15: Ares I US LH2 Tank Model Single Baffle Damping.

A baffle design using four rings in the Ares I US LH2 tank model is shown in Table 10. This series was added to our original testing plan to support the Orion Project, and is presented to show the validation of the analysis methodology for multiple baffles in a cylindrical tank. Test results and analysis for this design are shown in Table 11 and Figure 16. A nominal slosh wave amplitude test value of 1.00 inch ($\eta/R = 0.0464$) is reported in Table 10, and was used in the analysis plotted in Figure 16. This validates the assumption that in cylindrical tanks, for a given fill level, the damping contribution of multiple baffles can be added in series.

Table 10: Ares I US LH2 Tank Model Multiple Baffle Design.

| Baffle ID# | Baffle Width w/R | Baffle Location h/R |
|------------|--------------------|-----------------------|
| Orion #1 | 0.0533 | 2.04 |
| Orion #2 | 0.0533 | 1.77 |
| Orion #3 | 0.0533 | 1.50 |
| Orion #4 | 0.0533 | 1.24 |

Table 11: Ares I US LH2 Tank Model Multiple Baffle Damping.

| fill level h/R | FD TEST % critical damping ζ | FD TEST slosh wave amplitude η/R |
|---------------------|---|--|
| 1.30 | 1.76 | 0.0464 |
| 1.37 | 1.09 | 0.0464 |
| 1.44 | 0.904 | 0.0464 |
| 1.57 | 2.42 | 0.0464 |
| 1.64 | 1.52 | 0.0464 |
| 1.70 | 0.969 | 0.0464 |
| 1.84 | 2.09 | 0.0464 |
| 1.90 | 1.53 | 0.0464 |
| 1.97 | 1.02 | 0.0464 |
| 2.10 | 2.31 | 0.0464 |
| 2.17 | 1.41 | 0.0464 |
| 2.24 | 1.19 | 0.0464 |
| 2.30 | 0.639 | 0.0464 |

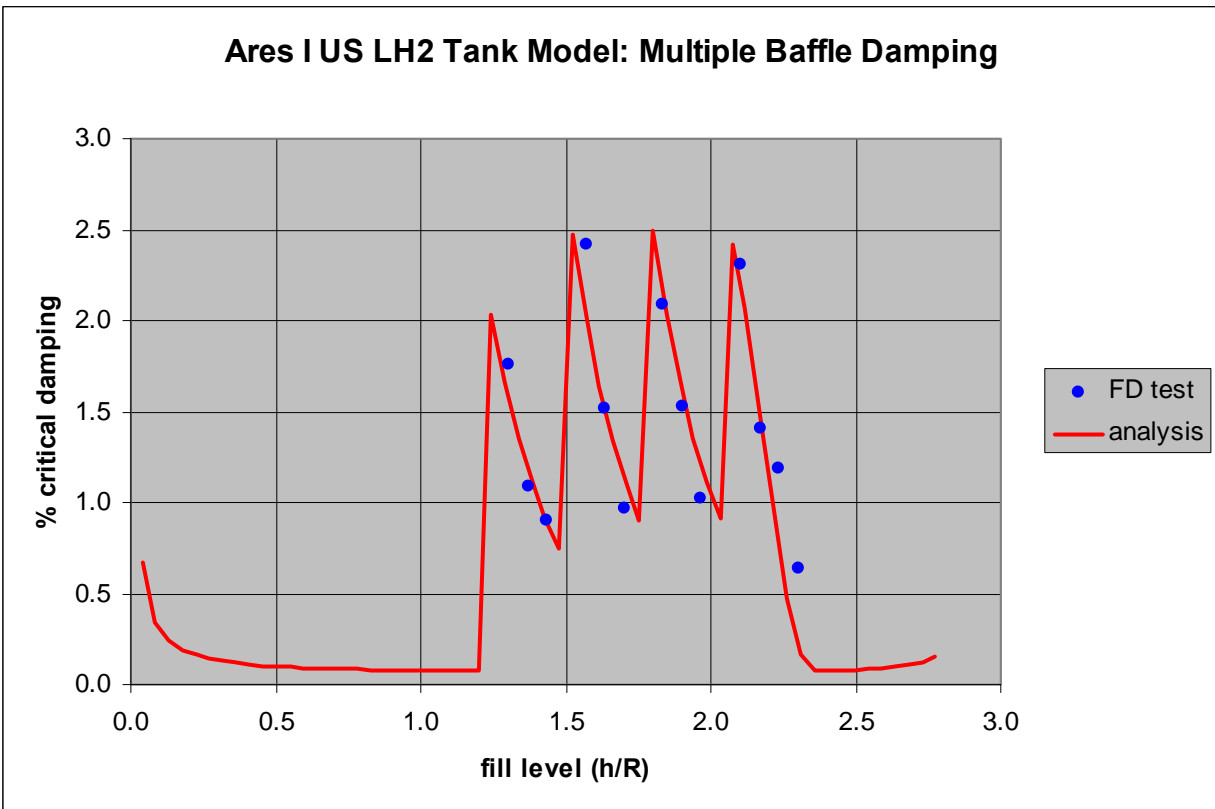


Figure 16: Ares I US LH2 Tank Model Multiple Baffle Damping.

ARES I US LOX TANK MODEL DIMENSIONS

The geometrical dimensions of the Ares I US LOX tank model used for the slosh dynamics analyses were measured directly from the tank and are shown in Figure 17. The tank model consists of a spherical lower dome of radius R , a barrel section, and a spherical cap upper dome of $1.16 R$ radius of curvature. The tank model was scaled approximately $1/5$ of the prototype dimensions, and was about 43 inches in diameter.

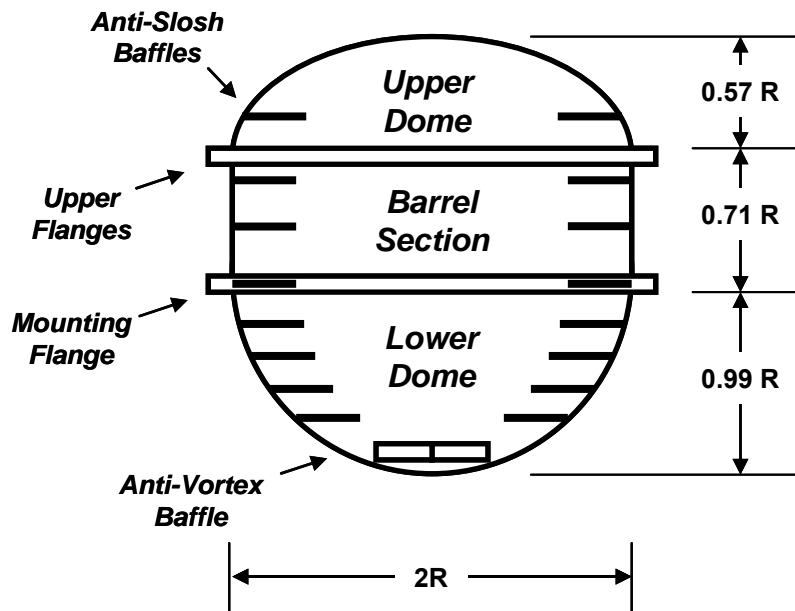


Figure 17: Ares I US LOX Tank Model Geometry.

ARES I US LOX TANK MODEL TESTING FOR SLOSH MODEL PARAMETERS

The slosh mechanical model parameters of slosh frequency, slosh mass, and pendulum hinge point location were obtained from random excitation (RE) tests performed on a bare tank (no baffles) (Parks, Lazor and Lacock 2011a).

The analysis and test results of the slosh mechanical model parameters of the Ares I US LOX tank model are summarized in Tables 12 through 17. The tables correspond to the non-dimensionalized first mode slosh frequency, first mode slosh mass, and first mode pendulum hinge point location, respectively. The test results are shown in Figures 18 through 20.

Apart from the frequency at the highest fill level, the comparison shows that all the parameters are within the margins used for stability analyses.

Table 12: Ares I US LOX Tank Model Slosh Frequency RE Test 1.

| fill level h/R | ANALYSIS slosh frequency $\omega_S (R/g)^{0.5}$ | RE TEST 1 slosh frequency $\omega_S (R/g)^{0.5}$ | difference (%) |
|--|---|--|---------------------------|
| 0.241 | 1.04 | 1.04 | 0.15 |
| 0.469 | 1.09 | 1.08 | 0.92 |
| 0.769 | 1.17 | 1.16 | 0.59 |
| 0.960 | 1.23 | 1.24 | 0.67 |
| 1.18 | 1.30 | 1.31 | 0.48 |
| 1.32 | 1.32 | 1.33 | 0.33 |
| 1.47 | 1.34 | 1.34 | 0.23 |
| 1.67 | 1.35 | 1.35 | 0.13 |
| 1.77 | 1.43 | 1.39 | 2.76 |
| 1.87 | 1.56 | 1.50 | 3.66 |
| 1.92 | 1.64 | 1.57 | 4.28 |
| 1.96 | 1.73 | 1.64 | 4.89 |
| 2.02 | 1.86 | 1.75 | 5.84 |

Table 13: Ares I US LOX Tank Model Slosh Frequency RE Test 2.

| fill level h/R | ANALYSIS slosh frequency $\omega_S (R/g)^{0.5}$ | RE TEST 2 slosh frequency $\omega_S (R/g)^{0.5}$ | difference (%) |
|--|---|--|---------------------------|
| 0.241 | 1.04 | 1.03 | 1.57 |
| 0.475 | 1.09 | 1.07 | 1.90 |
| 0.768 | 1.17 | 1.16 | 0.88 |
| 0.966 | 1.24 | 1.24 | 0.11 |
| 1.18 | 1.30 | 1.30 | 0.30 |
| 1.32 | 1.32 | 1.33 | 0.33 |
| 1.47 | 1.34 | 1.34 | 0.26 |
| 1.67 | 1.35 | 1.35 | 0.15 |
| 1.77 | 1.43 | 1.39 | 3.05 |
| 1.87 | 1.56 | 1.50 | 3.81 |
| 1.92 | 1.64 | 1.57 | 4.43 |
| 1.96 | 1.71 | 1.63 | 5.03 |
| 2.02 | 1.86 | 1.74 | 6.08 |

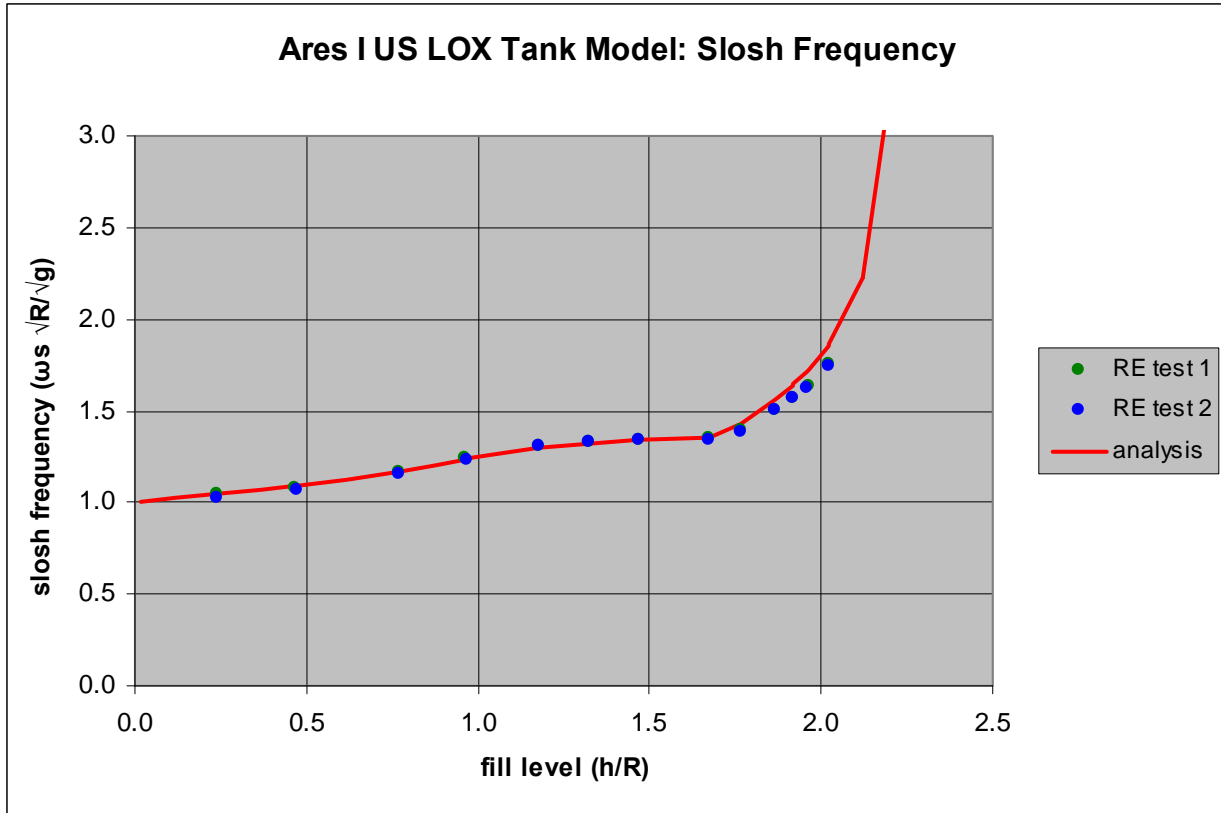


Figure 18: Ares I US LOX Tank Model Slosh Frequency.

Table 14: Ares I US LOX Tank Model Slosh Mass RE Test 1.

| fill level <i>h/R</i> | ANALYSIS slosh mass <i>m_s/m</i> | RE TEST 1 slosh mass <i>m_s/m</i> | difference (%) |
|--------------------------|--|---|-------------------|
| 0.241 | 0.916 | 0.849 | 7.25 |
| 0.469 | 0.827 | 0.860 | 4.07 |
| 0.769 | 0.695 | 0.701 | 0.82 |
| 0.960 | 0.601 | 0.592 | 1.36 |
| 1.18 | 0.496 | 0.490 | 1.09 |
| 1.32 | 0.436 | 0.439 | 0.69 |
| 1.47 | 0.388 | 0.389 | 0.12 |
| 1.67 | 0.335 | 0.335 | 0.13 |
| 1.77 | 0.290 | 0.292 | 0.71 |
| 1.87 | 0.231 | 0.225 | 2.71 |
| 1.92 | 0.201 | 0.199 | 0.61 |
| 1.96 | 0.172 | 0.175 | 1.60 |
| 2.02 | 0.135 | 0.136 | 0.70 |

Table 15: Ares I US LOX Tank Model Slosh Mass RE Test 2.

| fill level h/R | ANALYSIS slosh mass m_s/m | RE TEST 2 slosh mass m_s/m | difference (%) |
|---------------------|-----------------------------------|------------------------------------|-------------------|
| 0.241 | 0.916 | 0.873 | 4.63 |
| 0.475 | 0.824 | 0.813 | 1.44 |
| 0.768 | 0.695 | 0.713 | 2.54 |
| 0.966 | 0.597 | 0.562 | 5.85 |
| 1.18 | 0.495 | 0.512 | 3.26 |
| 1.32 | 0.436 | 0.452 | 3.51 |
| 1.47 | 0.388 | 0.399 | 2.74 |
| 1.67 | 0.335 | 0.311 | 7.17 |
| 1.77 | 0.290 | 0.283 | 2.57 |
| 1.87 | 0.232 | 0.232 | 0.08 |
| 1.92 | 0.200 | 0.194 | 3.23 |
| 1.96 | 0.177 | 0.182 | 2.91 |
| 2.02 | 0.136 | 0.139 | 2.13 |

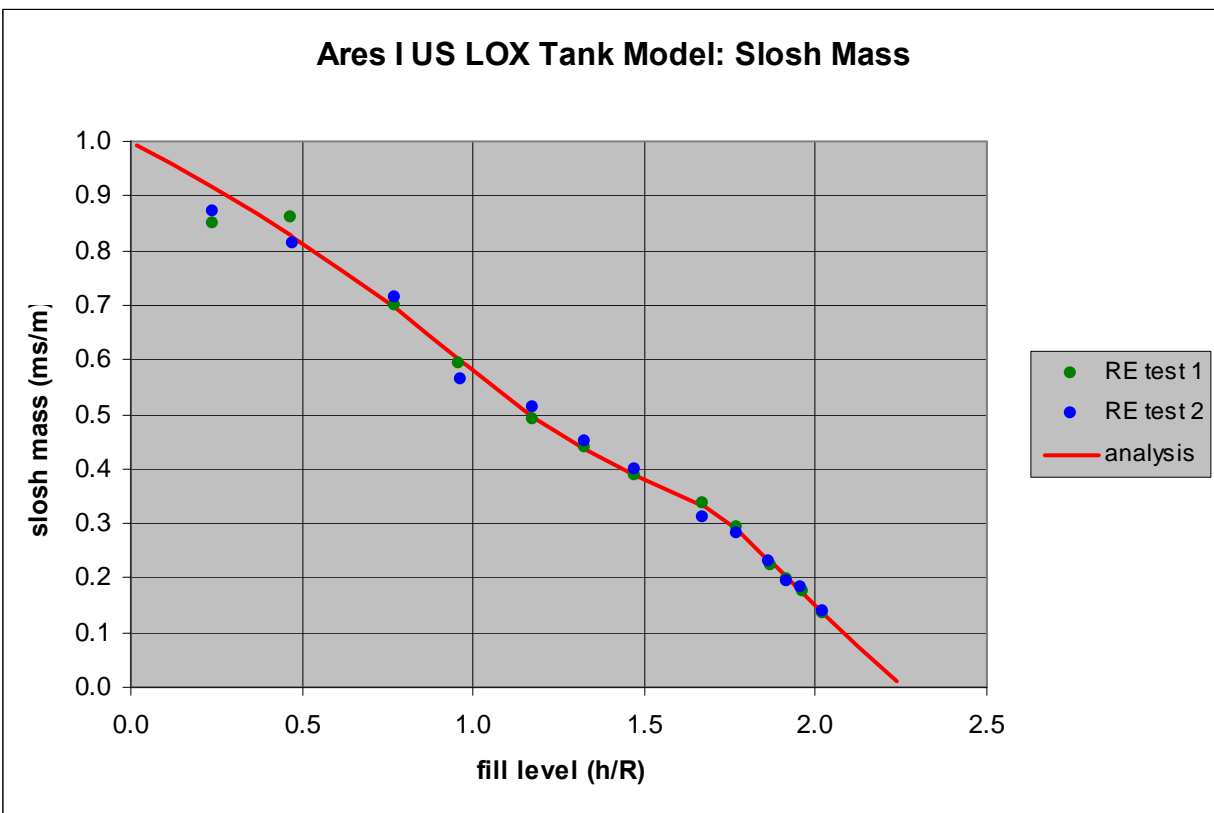


Figure 19: Ares I US LOX Tank Model Slosh Mass.

Table 16: Ares I US LOX Tank Model Pendulum Hinge Location RE Test 1.

| fill level <i>h/R</i> | ANALYSIS pendulum hinge point <i>H_s/R</i> | RE TEST 1 pendulum hinge point <i>H_s/R</i> | difference (%) |
|----------------------------------|---|--|---------------------------|
| 0.241 | 1.00 | 0.865 | 13.45 |
| 0.469 | 1.00 | 0.955 | 4.38 |
| 0.769 | 1.00 | 0.955 | 4.42 |
| 0.960 | 1.00 | 0.933 | 6.81 |
| 1.18 | 1.03 | 0.971 | 6.06 |
| 1.32 | 1.09 | 1.03 | 5.64 |
| 1.47 | 1.17 | 1.11 | 5.46 |
| 1.67 | 1.31 | 1.24 | 4.83 |
| 1.77 | 1.30 | 1.28 | 2.09 |
| 1.87 | 1.30 | 1.26 | 3.35 |
| 1.92 | 1.30 | 1.24 | 4.73 |
| 1.96 | 1.31 | 1.23 | 6.41 |
| 2.02 | 1.32 | 1.19 | 10.08 |

Table 17: Ares I US LOX Tank Model Pendulum Hinge Location RE Test 2.

| fill level <i>h/R</i> | ANALYSIS pendulum hinge point <i>H_s/R</i> | RE TEST 2 pendulum hinge point <i>H_s/R</i> | difference (%) |
|----------------------------------|---|--|---------------------------|
| 0.241 | 1.00 | 0.932 | 6.75 |
| 0.475 | 1.00 | 0.967 | 3.21 |
| 0.768 | 1.00 | 0.968 | 3.11 |
| 0.966 | 1.00 | 0.948 | 5.23 |
| 1.18 | 1.03 | 0.978 | 5.31 |
| 1.32 | 1.09 | 1.03 | 5.53 |
| 1.47 | 1.17 | 1.12 | 4.65 |
| 1.67 | 1.31 | 1.26 | 3.55 |
| 1.77 | 1.30 | 1.31 | 0.35 |
| 1.87 | 1.30 | 1.29 | 0.82 |
| 1.92 | 1.30 | 1.28 | 2.28 |
| 1.96 | 1.31 | 1.26 | 3.67 |
| 2.02 | 1.32 | 1.24 | 6.08 |

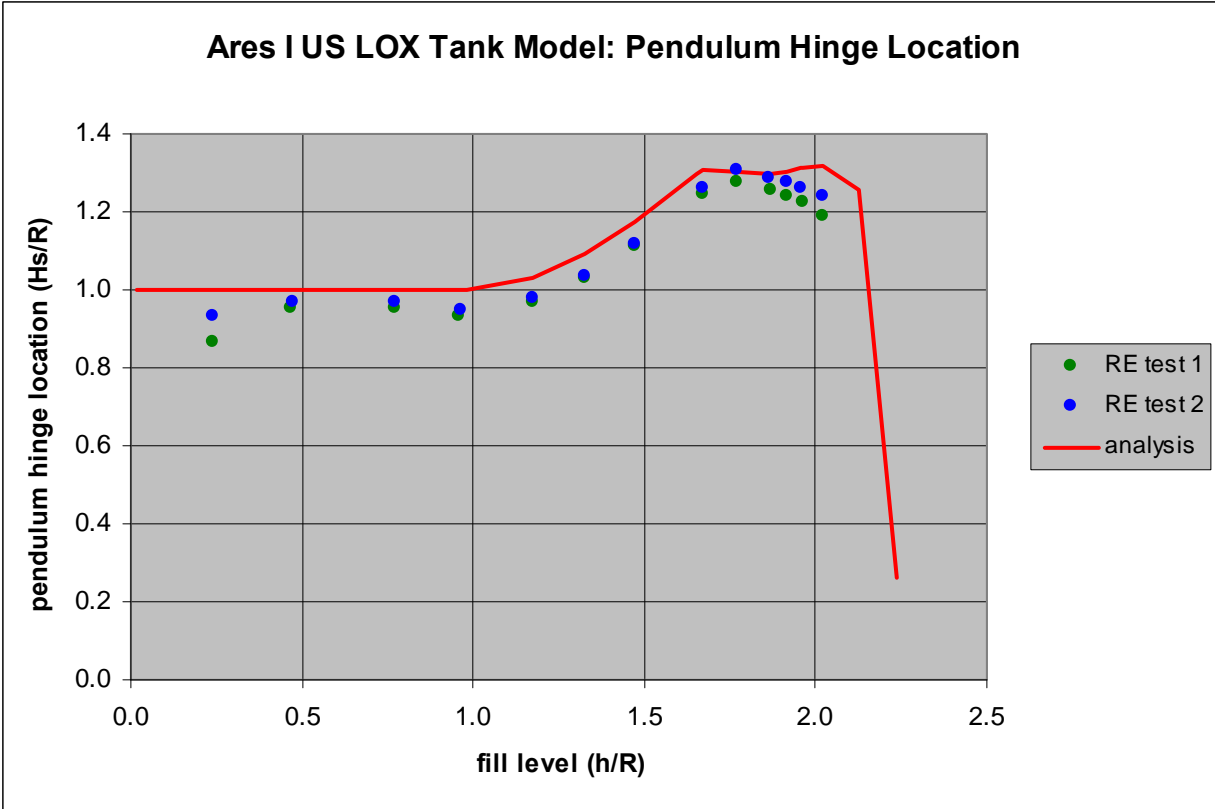


Figure 20: Ares I US LOX Tank Model Pendulum Hinge Location.

ARES I US LOX TANK MODEL TESTING FOR SMOOTH-WALL DAMPING

Free decay (FD) tests on the bare tank (no baffles) were performed to estimate smooth-wall damping. Test results and analysis are shown in Table 18 and Figure 21. The first test was performed for a nominal slosh wave amplitude of ½ inch ($\eta/R = 0.0229$), and the second for a nominal slosh wave amplitude of 1 inch ($\eta/R = 0.0458$). No significant difference in the measured smooth-wall damping was observed for the two slosh wave amplitudes tested.

Analytical values for this series were obtained from the smooth-wall damping equations for spherical tanks and cylindrical tanks (Equations 7 through 9). Test results show very good agreement with analytical values in the lower dome, although they are consistently higher than analytical values in the barrel section. No appreciable swirling of the fluid surface was reported for these series of tests (Parks, Lazor and Lacock 2011a).

Table 18: Ares I US LOX Tank Model Smooth-Wall Damping.

| fill level h/R | ANALYSIS % critical damping ζ_{sw} | FD TEST 1 % critical damping ζ | FD TEST 2 % critical damping ζ |
|---------------------|---|---|---|
| 0.241 | 0.290 | 0.324 | 0.330 |
| 0.472 | 0.147 | 0.165 | 0.163 |
| 0.768 | 0.0908 | 0.0976 | 0.0932 |
| 0.966 | 0.0722 | 0.0841 | 0.0814 |
| 1.18 | 0.0748 | 0.105 | 0.0976 |
| 1.32 | 0.0735 | 0.121 | 0.117 |
| 1.47 | 0.0726 | 0.121 | 0.124 |
| 1.67 | 0.0718 | 0.118 | 0.110 |
| 1.77 | 0.118 | 0.118 | 0.128 |
| 1.87 | 0.142 | 0.184 | 0.145 |
| 1.92 | 0.159 | 0.205 | 0.156 |

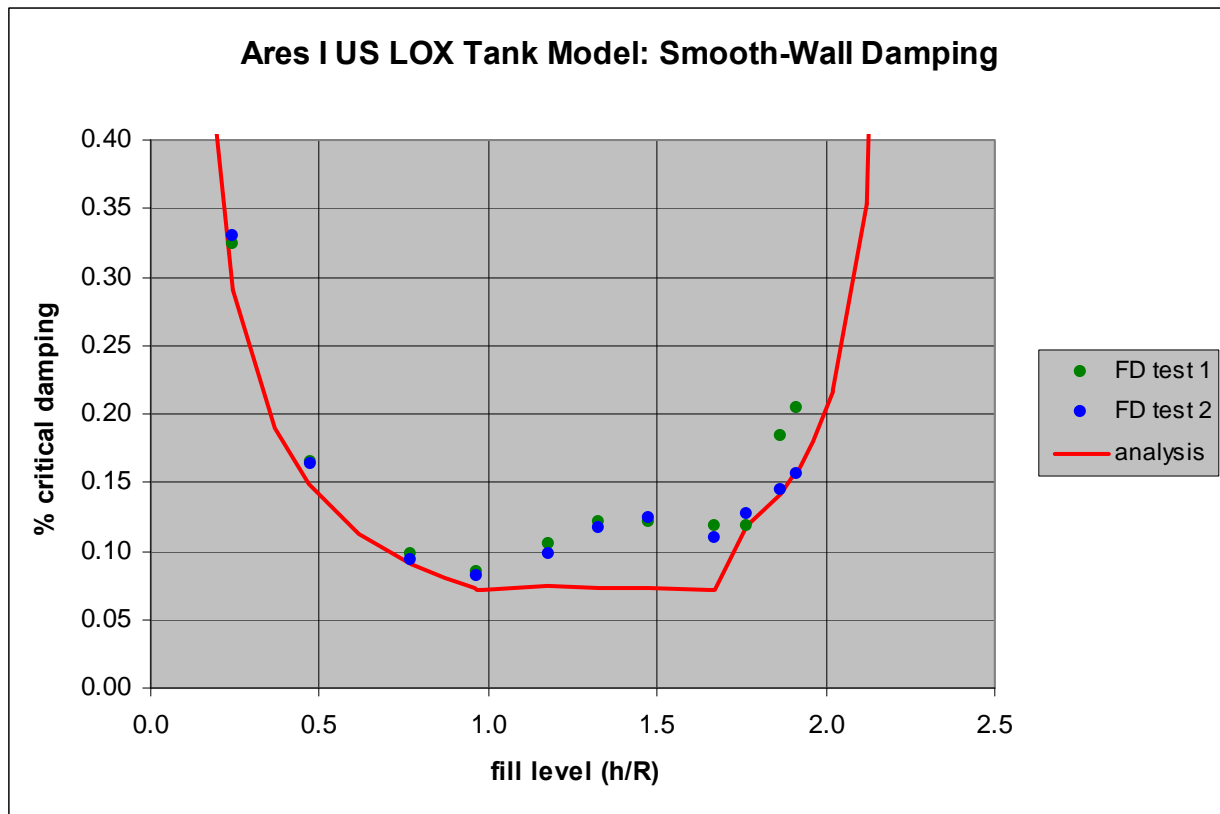


Figure 21: Ares I US LOX Tank Model Smooth-Wall Damping.

ARES I US LOX TANK MODEL TESTING FOR BAFFLE DAMPING

Free decay (FD) test results for a single baffle located in the barrel section of the tank, are shown in Table 20 and Figure 22. The baffle tested was 1.8 inches wide ($w/R = 0.0824$), and was located at a height of 27.85 inches ($h/R = 1.28$). Free decay (FD) test results for single baffle located in the lower dome of the tank, are shown in Table 21 and Figure 23. These configurations were tested to investigate the damping of single baffles in regions of different shapes within the tank.

The width and location of a multiple baffle configuration tested in the Ares I US LOX tank model is shown in Table 19 (Parks, Lazor and Lacock 2011a). Free decay (FD) test results for this configuration are shown in Table 22 and Figures 24 and 25. The average value of all the slosh wave amplitudes measured during testing of this configuration ($\eta/R = 0.0330$) was used in Miles equation (Equation 10) to create the analysis curves shown in Figures 24 and 25. The analysis curves of all the configurations presented in this section include the contribution of baffle damping (Equation 10) and smooth-wall damping (Equations 7 through 9).

It should be noticed that when the fill level was just over a baffle, test data usually showed higher values of damping than the ones predicted by analysis. This was particularly obvious in the multiple baffle configuration of the Ares I US LOX tank model. This may be explained by the fact that in Miles equation it is assumed that local flow in the neighborhood of a baffle is not affected by the free surface of the fluid (Stricklin and Baird 1966), when actually it is. During testing, when the fill level was very close to a baffle, the flow at the surface became very chaotic, developing splashing and breaking waves.

The agreement between test results and analysis is very good for the single baffle configurations. For the eight baffle configuration, the analysis curve shown in Figure 24 was made adding the damping contribution of each baffle in series, as is customary. The agreement between test and analysis appears to be good for fill levels located at the upper and lower domes. The agreement is not good for fill levels in the lower and middle regions of the barrel section, in the neighborhood of baffles #2 ($h/R = 1.55$), #4 ($h/R = 1.28$), and #6 ($h/R = 1.00$).

Table 19: Ares I US LOX Tank Model Anti-Slosh Baffles.

| Baffle ID# | Baffle Width w/R | Baffle Location h/R |
|-------------------|--------------------------------------|---|
| 1 | 0.147 | 1.85 |
| 2 | 0.147 | 1.55 |
| 4 | 0.147 | 1.28 |
| 6 | 0.147 | 1.00 |
| 7 | 0.147 | 0.781 |
| 8 | 0.147 | 0.572 |
| 9 | 0.147 | 0.357 |
| 10 | 0.156 | 0.181 |

Table 20: Ares I US LOX Tank Model Single Baffle Damping at the Barrel Section.

| fill level h/R | FD TEST % critical damping ζ | FD TEST slosh wave amplitude η/R |
|---------------------|---|--|
| 1.19 | 0.146 | 0.0479 |
| 1.23 | 0.642 | 0.0369 |
| 1.32 | 4.31 | 0.0297 |
| 1.37 | 2.21 | 0.0288 |
| 1.47 | 1.47 | 0.0371 |
| 1.67 | 0.707 | 0.0511 |

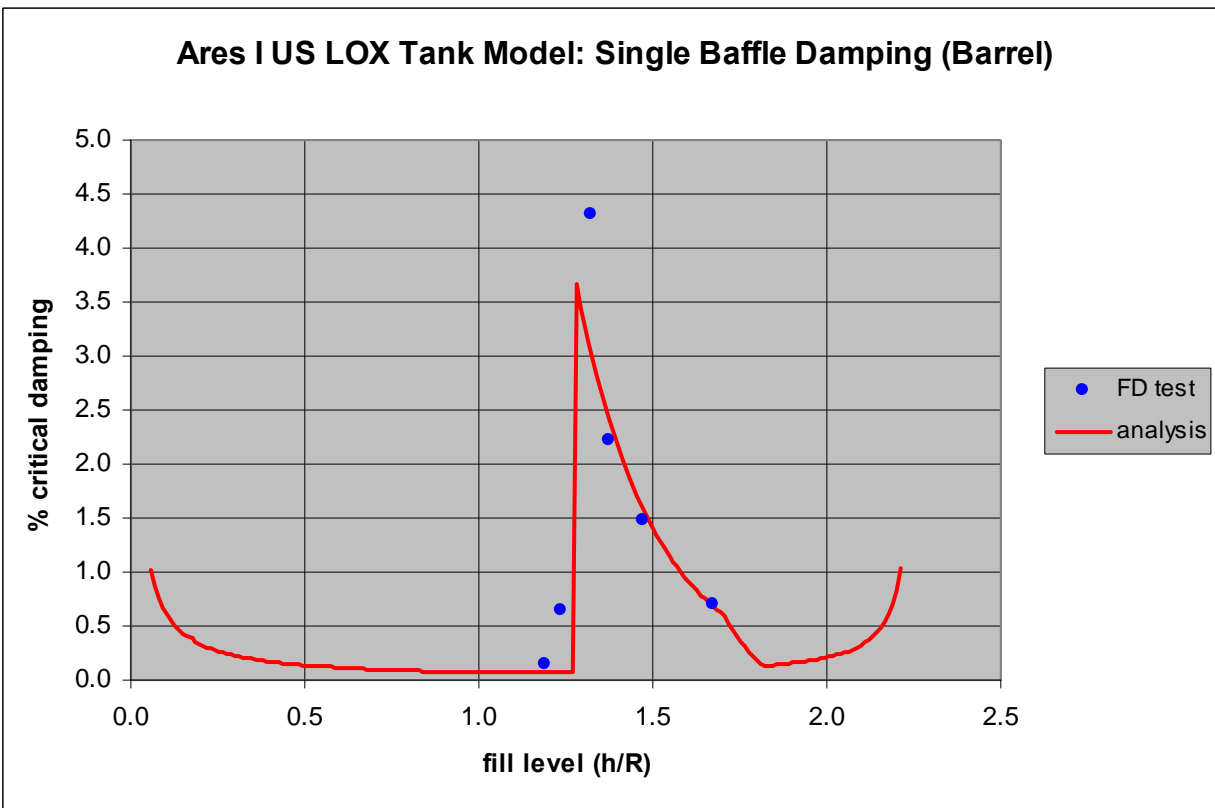


Figure 22: Ares I US LOX Tank Model Single Baffle Damping at the Barrel Section.

Table 21: Ares I US LOX Tank Model Single Baffle Damping at the Lower Dome.

| fill level h/R | FD TEST % critical damping ζ | FD TEST slosh wave amplitude η/R |
|---------------------|---|--|
| 0.49 | 0.285 | 0.0430 |
| 0.53 | 0.309 | 0.0586 |
| 0.62 | 11.5 | 0.0188 |
| 0.67 | 5.63 | 0.0348 |
| 0.77 | 2.61 | 0.0412 |
| 0.97 | 1.04 | 0.0423 |

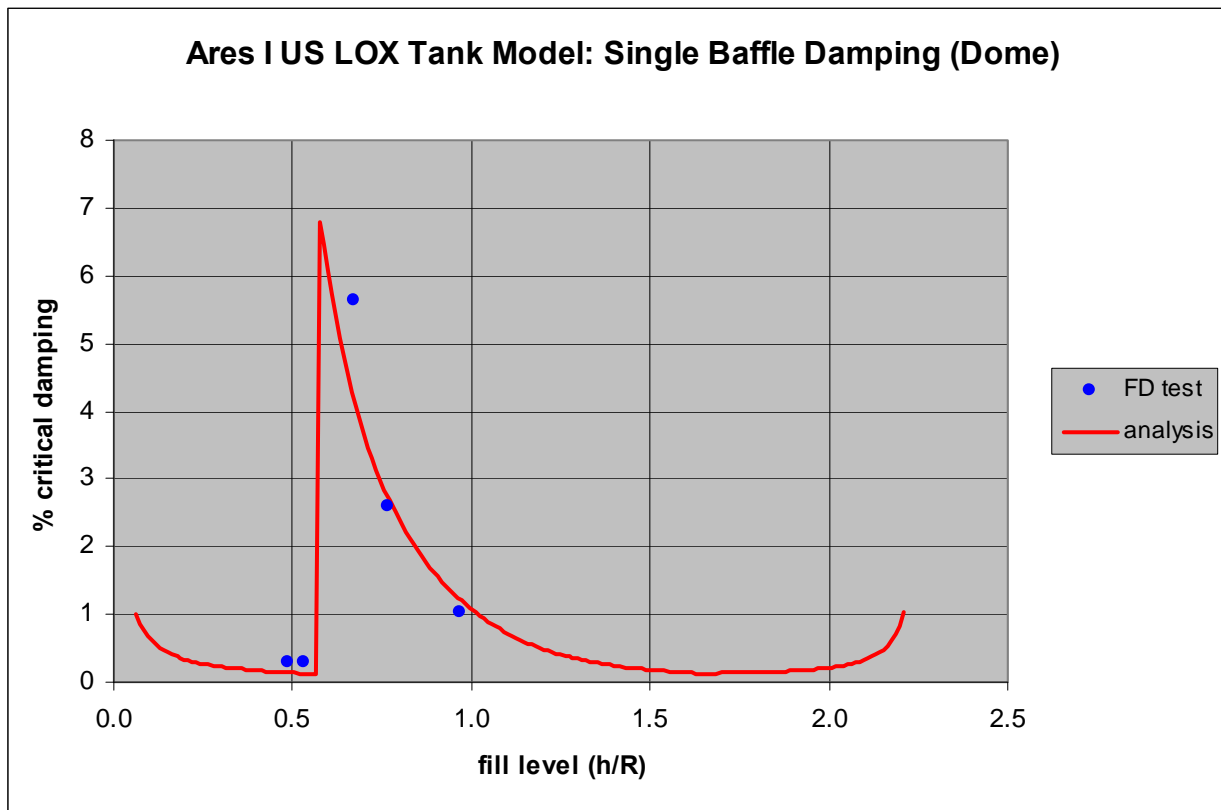


Figure 23: Ares I US LOX Tank Model Single Baffle Damping at the Lower Dome.

Table 22: Ares I US LOX Tank Model Multiple Baffle Damping.

| fill level h/R | FD TEST 1 % critical damping ζ | FD TEST 1 slosh wave amplitude η/R | FD TEST 2 % critical damping ζ | FD TEST 2 slosh wave amplitude η/R |
|--|--|---|--|---|
| 0.21 | 6.72 | 0.0105 | 5.18 | 0.00980 |
| 0.23 | 4.86 | 0.0178 | 7.23 | 0.0157 |
| 0.27 | 3.95 | 0.0256 | 3.09 | 0.0255 |
| 0.31 | 2.72 | 0.0312 | 3.09 | 0.0243 |
| 0.38 | 7.70 | 0.0182 | 9.97 | 0.0224 |
| 0.41 | 6.70 | 0.0207 | 6.52 | 0.0190 |
| 0.46 | 4.79 | 0.0354 | - | - |
| 0.52 | 3.29 | 0.0465 | 2.68 | 0.0363 |
| 0.60 | 15.74 | 0.0178 | - | - |
| 0.62 | 9.57 | 0.0303 | 10.78 | 0.0367 |
| 0.68 | 5.04 | 0.0361 | 4.40 | 0.0394 |
| 0.73 | 3.39 | 0.0435 | 2.75 | 0.0401 |
| 0.81 | 15.66 | 0.0318 | - | - |
| 0.83 | 6.85 | 0.0333 | 9.85 | 0.0455 |
| 0.86 | 6.33 | 0.0319 | - | - |
| 0.95 | 2.81 | - | 2.66 | - |
| 1.05 | 8.00 | 0.0458 | 10.06 | - |
| 1.11 | 4.64 | 0.0335 | - | - |
| 1.14 | 3.26 | 0.0412 | 3.73 | 0.0423 |
| 1.22 | 2.52 | 0.0467 | 2.21 | 0.0399 |
| 1.30 | 22.90 | 0.0274 | - | - |
| 1.32 | 9.64 | 0.0352 | - | 0.0403 |
| 1.37 | - | - | 5.52 | 0.0591 |
| 1.41 | 4.18 | 0.0387 | 3.67 | 0.0535 |
| 1.50 | 2.16 | 0.0000 | 2.31 | 0.0402 |
| 1.57 | 20.56 | 0.0128 | - | - |
| 1.60 | 8.64 | 0.0252 | 10.61 | 0.0407 |
| 1.67 | 4.44 | 0.0533 | 4.16 | 0.0430 |
| 1.73 | 3.03 | 0.0416 | - | - |
| 1.80 | 1.74 | 0.0358 | 2.09 | 0.0366 |
| 1.88 | 11.73 | 0.0218 | - | - |
| 1.90 | 15.73 | 0.0162 | - | - |
| 1.95 | 2.30 | 0.0324 | 2.99 | 0.0292 |
| 2.01 | 1.21 | 0.0342 | 1.50 | 0.0336 |
| 2.06 | 0.78 | 0.0370 | 0.65 | 0.0266 |

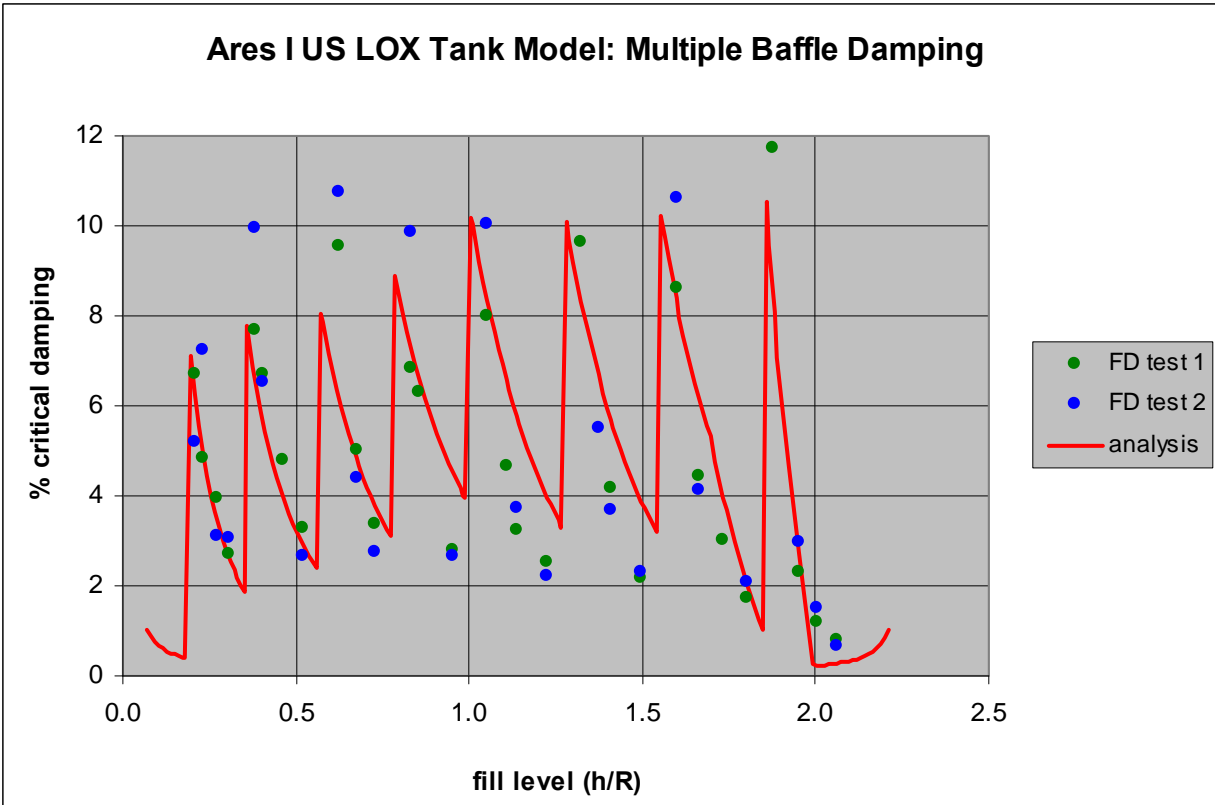


Figure 24: Ares I US LOX Tank Model Multiple Baffle Damping (Analysis Curve Assuming Damping Added in Series).

If the damping contribution of the baffles located in the barrel section and the upper dome of the tank (baffles #1, #2, #4, and #6) was considered individually (rather than in series), the analytical curve would produce a better match with the test results, as shown in Figure 25.

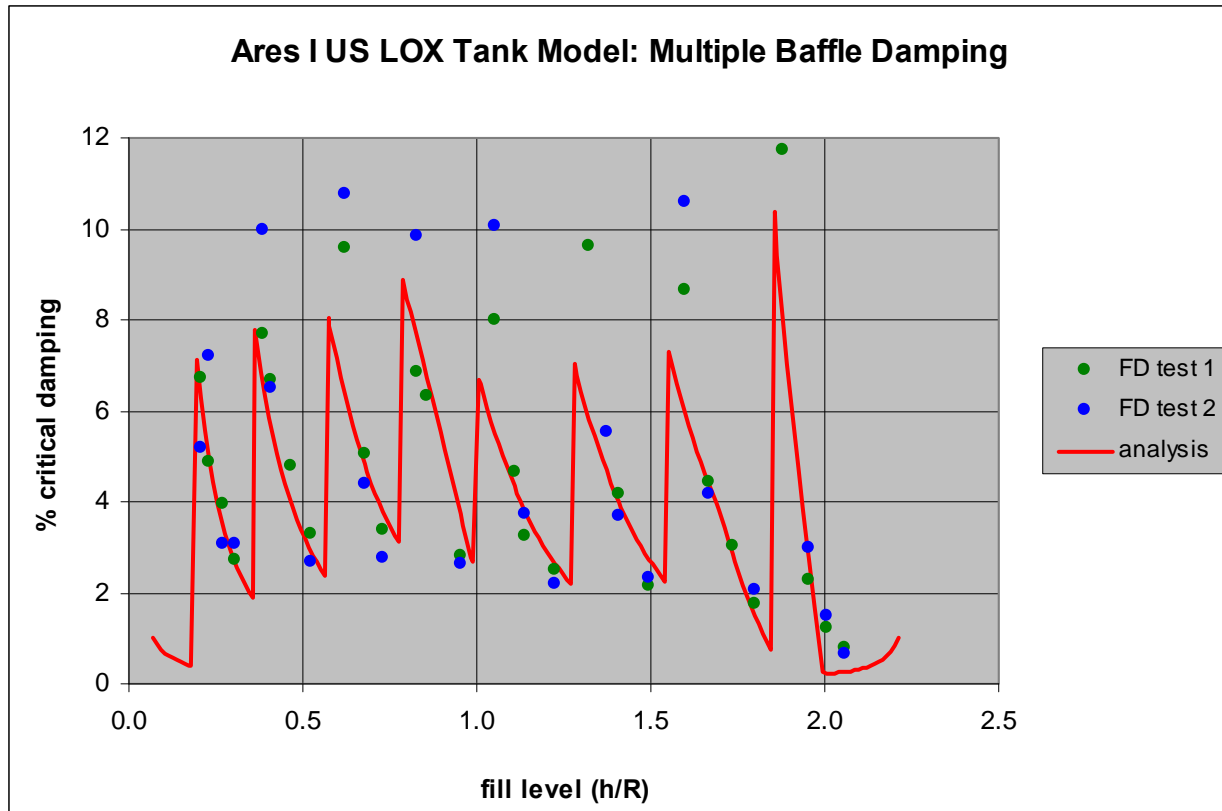


Figure 25: Ares I US LOX Tank Model Multiple Baffle Damping (Analysis Curve Assuming Only Individual Baffle Damping for the Middle and Upper Regions of the Tank).

CONCLUSIONS

The slosh linear mechanical model used for the Ares I US LOX and LH2 tanks has been validated by using lateral slosh testing. Random excitation tests were performed to obtain the parameters of the model: slosh frequency, slosh mass, and pendulum hinge point location. The agreement between test results and analysis was good and within the expected ranges.

Free decay tests were performed to obtain smooth-wall damping and baffle damping. Smooth-wall damping is independent of the slosh wave amplitude for the small slosh wave amplitude magnitudes tested, as expected from historical data (Abramson et al. 1966). Test results and analyses compared very well in the Ares I US LH2 tank model, and in the lower dome of the Ares I US LOX tank model.

Miles equation for baffle damping was also validated from these tests. Single and multiple baffle configurations were tested in the different regions of the tanks: spherical (domes) and cylindrical (barrel). The form of Miles equation presented in Equation 10 proved to be very accurate predicting baffle damping, even in challenging regions, such as the tank domes. Analyses and test results compared very well for the single baffle configurations tested. The match was also very good for the multiple baffle configurations in the barrel section of the Ares I US LH2 tank model and the hemispherical dome of the Ares I US LOX tank model. This was not the case with

the baffles located in the barrel section of the Ares I US LOX tank model. The test results appear to indicate that, for a tank of the shape of the Ares I US LOX tank model, the influence of the baffles located in the lower dome is negligible in the middle and upper regions of the tank. Further testing should be performed to confirm this.

REFERENCES

Anonymous, "Propellant Slosh Loads": NASA SP-8009 (1968).

Abramson, H. Norman, "Slosh Suppression": NASA SP-8031 (1969).

Abramson, H. Norman, ed., "The Dynamic Behavior of Liquid in Moving Containers": NASA SP-106 (1966).

Abramson, H. Norman, and Guido E. Ransleben, "Simulation of Fuel Sloshing Characteristics in Missile Tanks by Use of Small Models", *American Rocket Society Journal* 30, no. 1 (1960): 603-613.

Bugg, Frank, "Evaluation of Flexible Ring Baffles for Damping Liquid Oscillations": NASA TM X-64730 (1973).

Bugg, Frank M., "X-33 Slosh Model Parameter Tolerances": NASA Marshall Space Flight Center (1997): Memorandum ED23-97-063.

Dodge, Franklin T., "The New Dynamic Behavior of Liquids in Moving Containers": Southwest Research Institute (2000).

Dodge, Franklin T. and H. Norman Abramson, "Liquid Propellant Dynamics in the Saturn/Apollo Vehicles – A Look Back": *American Institute of Aeronautics & Astronautics* (2000): AIAA 2000-1676.

Dodge, Franklin T. and Luis R. Garza, "Equivalent Mechanical Model of Propellant Sloshing in the Workshop Configuration of the Saturn S-IVB": NASA CR-102615 (1969).

Ibrahim, Raouf A., "Liquid Sloshing Dynamics: Theory and Applications": Cambridge University Press (2005).

Green, S., D. Walter, and R. Burkey, "Lateral Slosh Test for Stereo Propellant Tank" Final Report: SwRI Project 18.11632.01.008 (2005).

Keulegan, G. H., and L. H. Carpenter, "Forces on Cylinders and Plates in an Oscillating Fluid": NBS Report 4821 (1956).

Mason, Paul A. C. and Scott R. Starin, "Propellant Slosh Analysis for the Solar Dynamics Observatory": Goddard Spaceflight Center (2005).

Miles, J. W., “Ring Damping of Free Surface Oscillations in a Circular Tank”, *ASME Journal of Applied Mechanics* 25 (1958): 274-276.

Parks, Russel A., Daniel R. Lazor, and Adam T. Lacock, “Ares I 1/5 Scale LOX Tank Lateral Slosh Test Report”: ARES1-DEV-09-060 (2011a).

Parks, Russel A., Daniel R. Lazor, and Adam T. Lacock, “Ares I 1/5 Scale LH2 Tank Lateral Slosh Test Report”: ARES1-DEV-09-070 (2011b).

Parks, Russel A., Daniel R. Lazor, and Adam T. Lacock, “Orion Service Module Lateral Slosh Test Report”: ORION-DEV-10-026 (2011c).

Roberts, James R., Eduardo R. Basurto, and Pei-Ying Chen, “Slosh Design Handbook I”: Northrop Space Laboratories (1964).

Silveira, Milton A., David G. Stephens and H. Wayne Leonard, “An Experimental Investigation of the Damping of Liquid Oscillations in Cylindrical Tanks with Various Baffles”: NASA TN D-715 (1961).

Stephens, David G., H. Wayne Leonard, and Milton A. Silveira, “An Experimental Investigation of the Damping of Liquid Oscillations in an Oblate Spheroidal Tank with and without Baffles”: NASA TN D-808 (1961).

Stricklin, G. P. and J. A. Baird, “A Survey of Ring Baffle Damping in Cylindrical Tanks”: NASA TN R-185 (1966).

Sumner, Irving E., D. J. Shramo, and Andrew J. Stofan, “Experimental Sloshing Characteristics and a Mechanical Analogy of Liquid Sloshing in a Centaur Liquid Oxygen Tank”: NASA TM X-999 (1964).

Unruh, J. F., D. D. Kana, F. T. Dodge, and T. A. Fey, “Digital Data Analysis Techniques for Extraction of Slosh Model Parameters”, *Journal of Spacecraft and Rockets*, Vol. 23 (1986): 171.

BIOGRAPHIES

José G. Pérez, BS Mechanical Engineering, University of Puerto Rico, MS Civil Engineering, University of Puerto Rico, MS Aerospace Engineering, Virginia Polytechnic Institute and State University. He has fifteen years of research and development experience in aerospace related fields, including lunar soil simulants, composite materials, impact dynamics, and slosh dynamics. He has been working at NASA Marshall Space Flight Center for eight years, where he has been the slosh dynamics lead of the Dynamics, Loads and Strength Branch. He has worked as a slosh dynamics engineer on the Ares I Launch Vehicle and the Space Launch System. He is a member of the Planetary Society.

Russel A. Parks, BS Mechanical Engineering Auburn University (1992) and MS in Engineering University of Alabama in Huntsville (1996), is Modal Team lead in the Structural Dynamics Test

Branch of Marshall Space Flight Center. He has eighteen years of experience in the area of structural dynamics test. In that time frame, he has participated in and led a multitude of test programs related to space launch vehicles, components, and payloads development and verification. More recently he helped develop a new slosh dynamics test facility in support of the NASA Constellation program. This facility has also been used in slosh dynamics research related to other space related projects.

Daniel R. Lazor, BS/MS Mechanical Engineering, University of Cincinnati, is currently working in the Structural Dynamics Test Branch at Marshall Space Flight Center. Prior to joining NASA, he worked as a research assistant at the University of Cincinnati's Structural Dynamics Research Laboratory, where he performed acoustic and structural dynamics testing on a variety of automotive, aquatic, civil infrastructure, and aerospace components and vehicles. Currently, he is working to integrate image processing techniques to facilitate fluid slosh analysis, and continues work to test and develop techniques to improve testing and analysis for a variety of structures.